Physical Modeling of Wind Turbine Generators

In a Small Scale Analog System

By

Xuntuo Wang

B.S., Electrical Engineering
General Motors Institute, 2012

Submitted to the
Department of Electrical Engineering and Computer Science
In Partial Fulfillment of the Requirements for the Degree of

Master of Science

at the

Massachusetts Institute of Technology

June 2014

Signature of Author .... Signature redacted .....

Department of Electrical Engineering and Computer Science

May 23, 2014

Certified by ..... Signature redacted .....

James L. Kirtley, Jr.

Professor, Department of Electrical Engineering and Computer Science

Accepted by ..... Signature redacted .....

Leslie A. Kolodziejski

Chair, EECS Committee on Graduate Students

Physical Modeling of Wind Turbine Generators
In a Small Scale Analog System

By
Xuntuo Wang

Submitted to the
Department of Electrical Engineering and Computer Science
In Partial Fulfillment of the Requirements for the Degree of
Master of Science

Abstract

This project represents the physical modeling and experimental test of a Doubly-fed Induction Machine (DFIM), in order to substantially analyze the characteristic behaviors of wind turbines and its use in the micro-grid network.

The environment set-up is based on a smart micro-grid system, which consists of the grid, a diesel generator, a solar panel, and a wind farm. The hardware work includes the design of a 2.5kW inverter and a L-C-L grid filter (including inductor design and construction).

The goal of this research is to better emulate the operation principles of wind turbine system. Future work proposes developing a better control method to improve the stability and reliability of the wind turbine system.

Keywords: DFIM, micro-grid, space vector PWM, DTC-SVM, back-to-back inverter, inductor design, and grid filter.

Thesis Supervisor: Prof. James L. Kirtley, Jr.

Title: Professor of Electrical Engineering

Acknowledgements

I would like to thank my thesis advisor Professor James L. Kirtley Jr. and academic supervisor Professor Jeffrey Lang for their enormous guide and supports throughout the entire project.

I would like to thank Dr. Mingguo Zhao of Tsinghua University and Dr. Jimmy Peng of Masdar Institute of Science and Technology for their help on the inductor building process.

I would like to thank my labmate Arijit Banerjee for his generous guidance on the Doubly-Fed Induction Machine modeling, and Jorge and Ben's work on the software interface and micro-grid set-up.

This project is financially supported by Masdar Institute of Science and Technology, Abu Dhabi, United Arab Emirates.

TABLE OF CONTENTS

LIST OF FIGURES

LIST OF TABLES

Chapter 1 INTRODUCTION

1.1 Motivation

Since the beginning of 20th century, the principal source of energy for electricity generation has been gradually shifted from the traditional coal power plant to the renewable energy section. In the era of rapid development of renewable energy, wind energy makes up a large portion, with an expected percentage of 25% for the U.S. market in 2025 [1].

(a) Traditional coal power plant.

(b) Siemens on-shore and off-shore wind plants.

Figure 1. Traditional coal energy and wind energy.

As indicated in figure 2 of the U.S. Electric Resource Mix, wind energy has been playing a critical role. Wind energy penetration (%) is defined as the total amount of wind energy produced annually divided by the gross annual electricity demand (TWh). According to the DOE, the wind energy penetration level in the US reached 1.9% by 2008, with highest state levels in Iowa 13.3%, Minnesota 10.4% and Texas 5.3%. The worldwide wind energy penetration by 2008 was 1.5% [1].

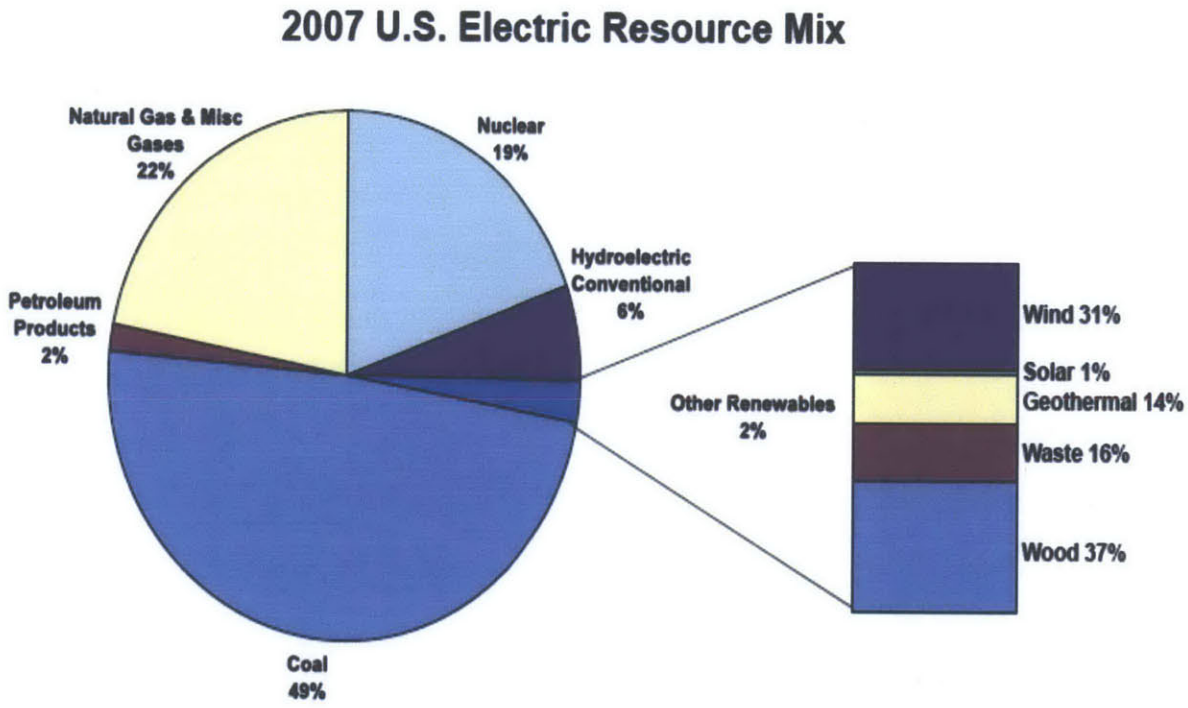

Figure 2. Breakdown chart of the U.S. Electric Resource Mix in 2007.

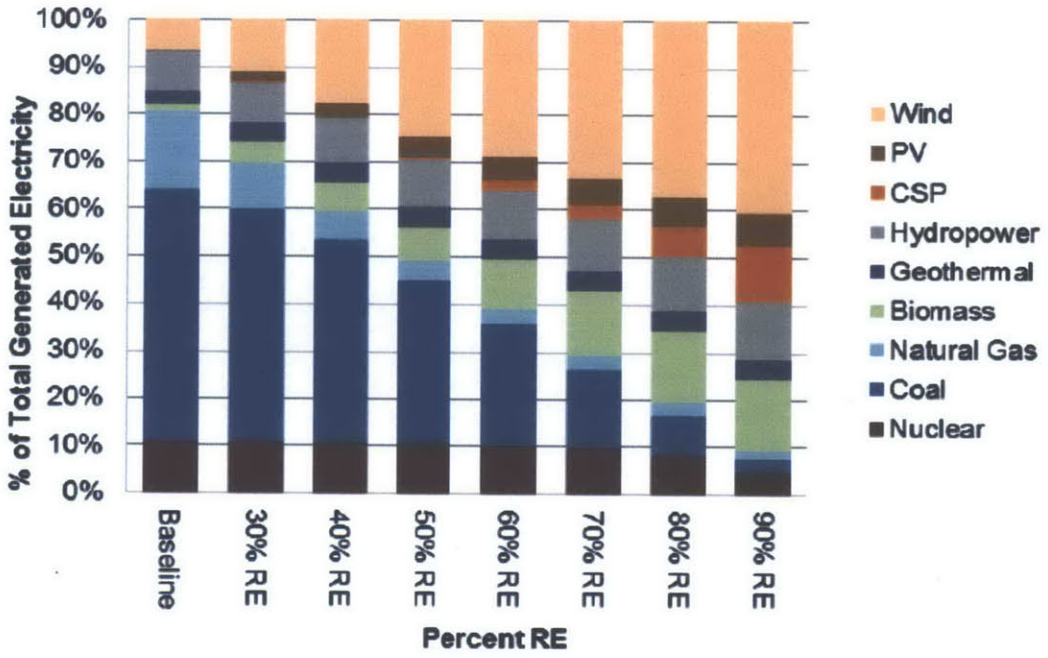

Figure 3. U.S Generation Mix for Different Renewable Penetration (RE) in 2050.

Figure 3 shows the historical development of Danish electricity system from a few central power plants 30 years ago to thousands of small, decentralized units today.

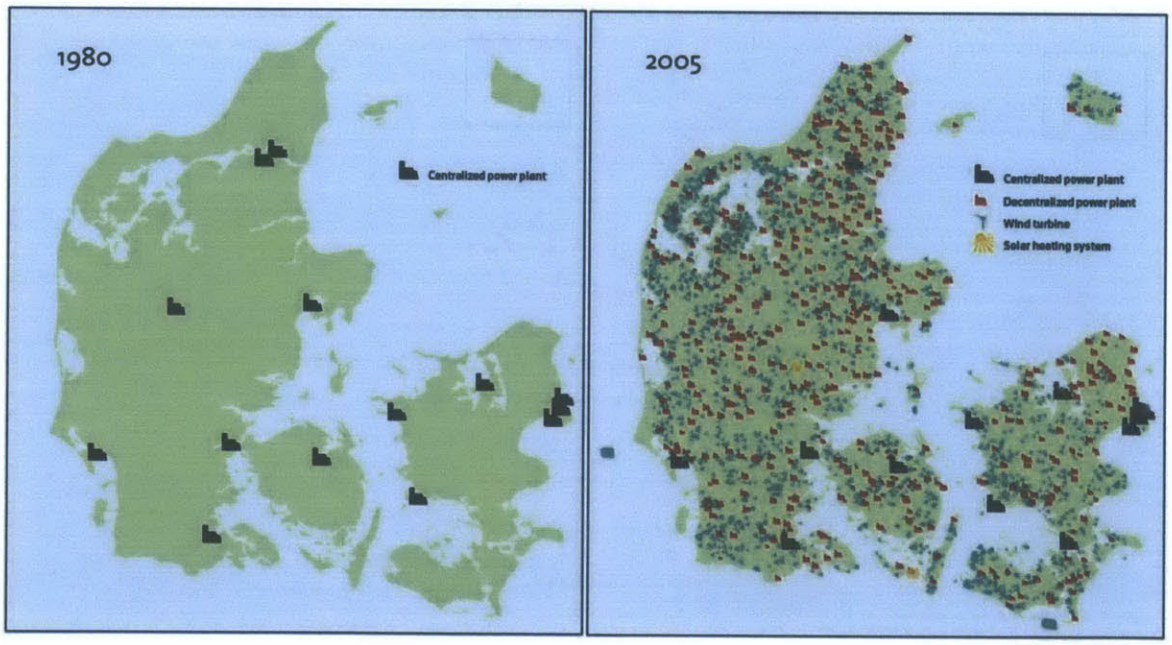

Figure 4. Historical development in the Danish electricity system.

In the wind turbine system, much attention has been paid to its stability and dynamics due to the changing wind speed and unpredictable electric system shut-down. These are the main technical difficulties of the Doubly-fed Induction Machines (DFIM) in the wind-turbine application. Therefore, my research work at RLE proposes to present a deep analysis on these addressed issues with the physical modeling of DFIM in a small scale analog system. This research work is conducted in a micro-grid environment.

1.2 Micro-grid environment

The micro-grid environment mainly comprises of four separate systems: the grid, solar, wind, and diesel generator as shown in figure 6. This project is in a collaboration with Masdar Institute of Science and Technology, Abu Dhabi, UAE.

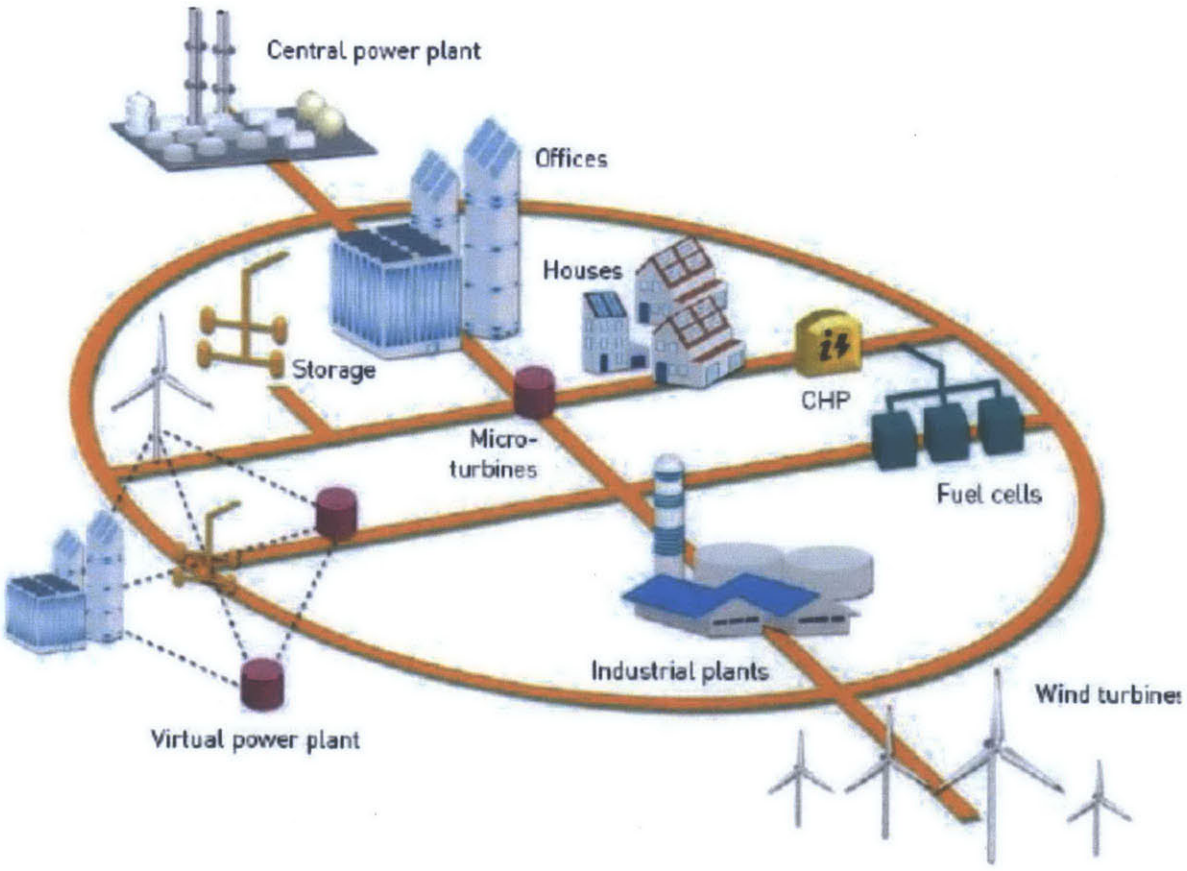

Figure 5. Interaction with consumers at the local level.

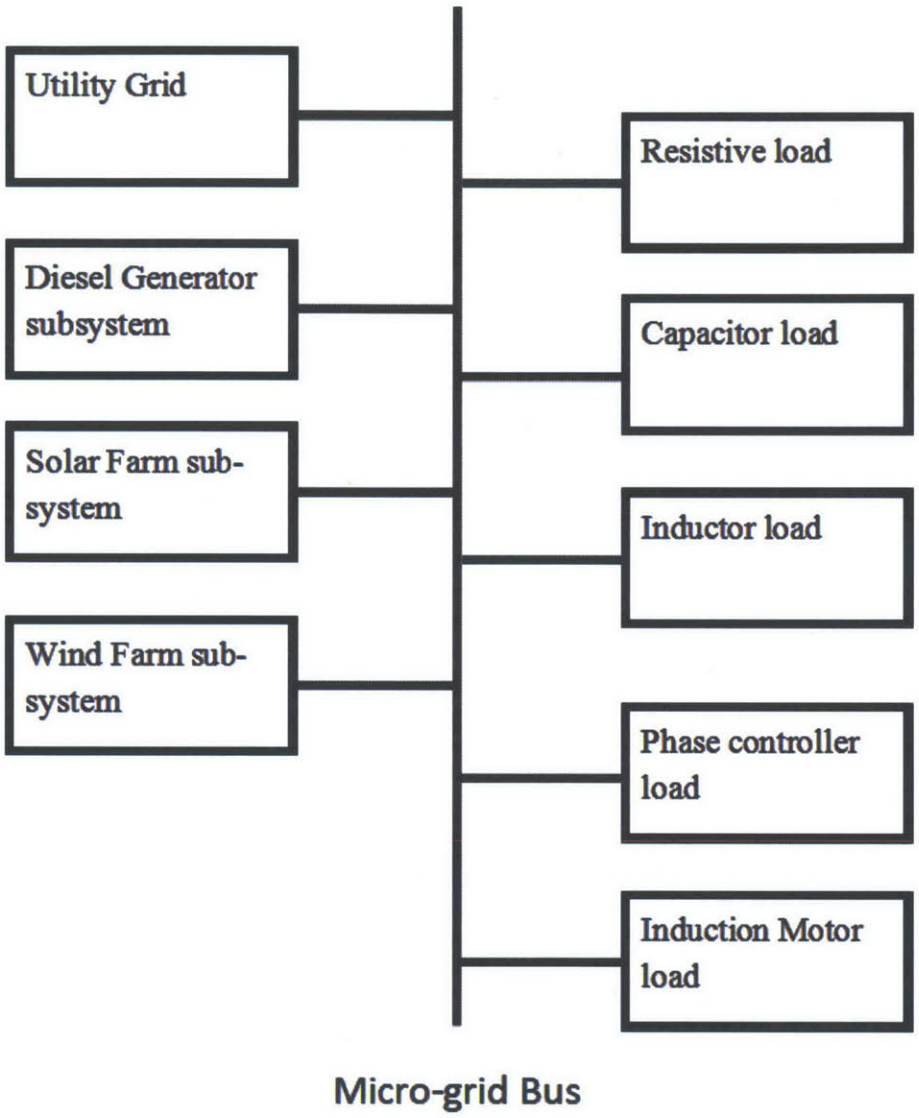

Figure 6(a). Micro-grid system diagram.

- *Resistive loads*

The resistive loads are constructed from six large, high-power ceramic resistors. Each resistive load is a Y configuration of three resistors, with each resistor tuned to 48 ohms, thus providing two resistive loads of 900 watts each. Each group of three resistors can be accessed by one relay so effectively we have two independent resistive loads.

Figure 6(b). Resistive load.

- *Inductive load*

The inductive load is constructed from three laminated iron cores. Each core has two air gaps and 270 windings to provide an inductance of approximately 108 mH. At our line voltage, this provides a total inductive load of about 1.05 kVAR.

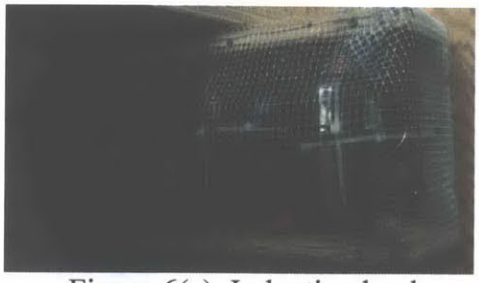

Figure 6(c). Inductive load.

- *Capacitive load*

The capacitive load is constructed from six large AC capacitors of 80μF. These are connected in a Y configuration with two capacitors in each leg connected in series to provide 40μF per leg. At our line voltage, this provides a total capacitive load of about 650 VAR.

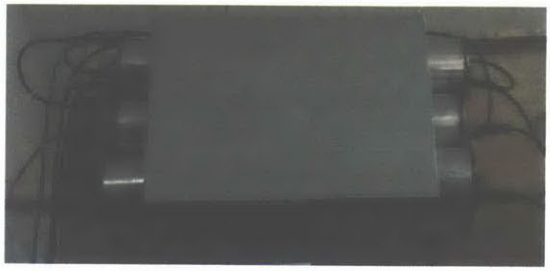

Figure 6(d). Capacitive load.

- *Phase-controlled load*

The phase-controlled load is constructed from three single-phase light dimmers, mounted side to side with the levers mechanically coupled. Each of these dimmers is connected in series to a 60-watt incandescent light bulb, and the dimmer/light bulb pairs are connected in a Y configuration with the neutral point connected to the neutral line of the micro-grid. This configuration provides a total phase-controlled load of up to 180 watts.

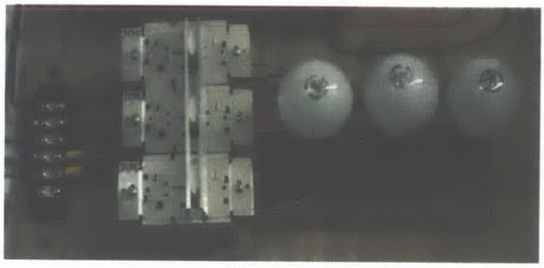

Figure 6(e). Phase controller load.

- *Induction motor load*

A 1-HP squirrel cage induction motor and a 1.5-HP DC motor were purchased and their shafts were mechanically coupled. The induction motor is connected to the micro-grid bus through an electromechanical switch and can be connected and disconnected like the other loads. The DC motor output is connected to a resistor so that the torque loading on the motor can be adjusted by varying the effective resistor. Currently the resistor has a fixed value, but it has been planned to include a controller to make the IM loading variable.

Figure 6(f). Inductor motor load.

- Diesel Generator and its power electronics drive

A diesel generator with 460V/2.3A rating was purchase and connected to the micro-grid. A buck converter and communication system has been built, providing the power to both DC motor and induction machine.

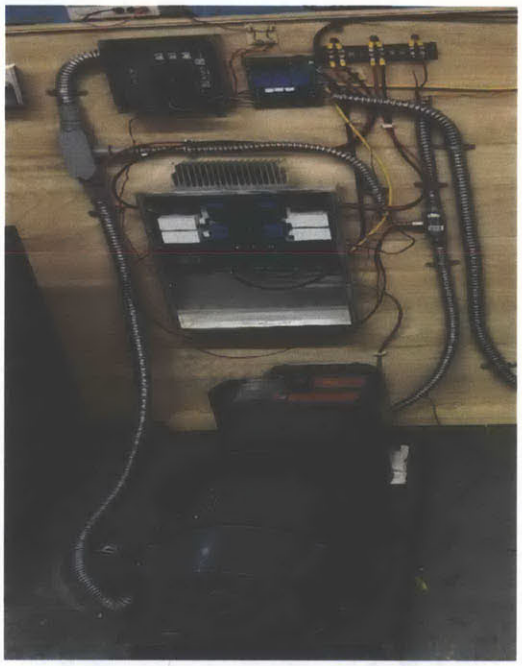

Figure 6(g). Diesel Generator and its power electronics drive.

The wind farm is a small-scale emulator of electrical system of a wind turbine, consisting a DC motor and slip ring motor operate as a synchronous mahcine. In DFIM, the slip rings are used to supply external power to the rotor to achieve the wide-range speed control.

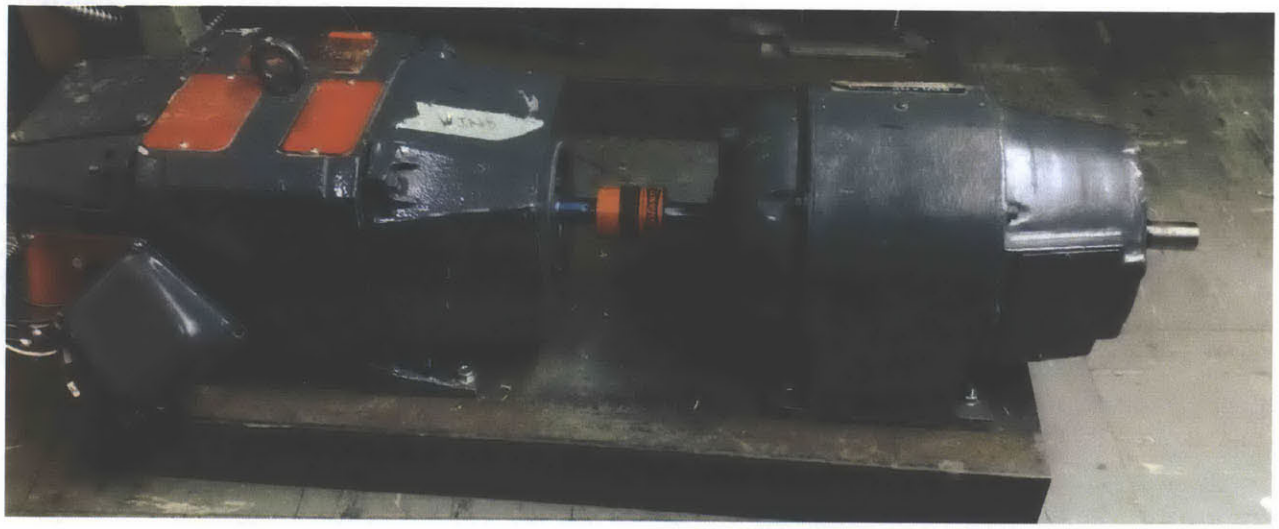

Figure 6(h). Wind Farm Emulator (DC motor on the left, slip ring motor on the right).

In order to drive this three-phase wound-rotor induction machine, a back-to-back converter is designed and constructed to feed power from the rotor to the grid when the machine operates at super-synchronous speed, and feed power from the grid to the rotor when the machine operates at sub-synchronous speed.

1.3 Overview

This thesis is divided into three main parts: system modeling, control algorithm, and hardware implementation. Chapter 2 introduces the system modeling of the analog system for DFIM. Chapter 3 describes three control methods: Space Vector Modulation: Direct Torque Control, and Field Orientated Control. The DTC-SVM and Stator-flux FOC are examined to be the optimum control techniques for DFIM. Chapter 4 details the hardware work including the construction of a 2.5kW DC/AC inverter and a grid L-C-L filter. Chapter 5 presents an initial test on the machine drive system. Chapter 6 summarizes the research work done thus far and proposes the future work.

Chapter 2 SYSTEM MODELING

2.1 Block Diagram

The wind turbine electrical system including the doubly-fed induction machine, electrical circuitry, and rotor, as shown in the figure below, connects to the mechanical blades.

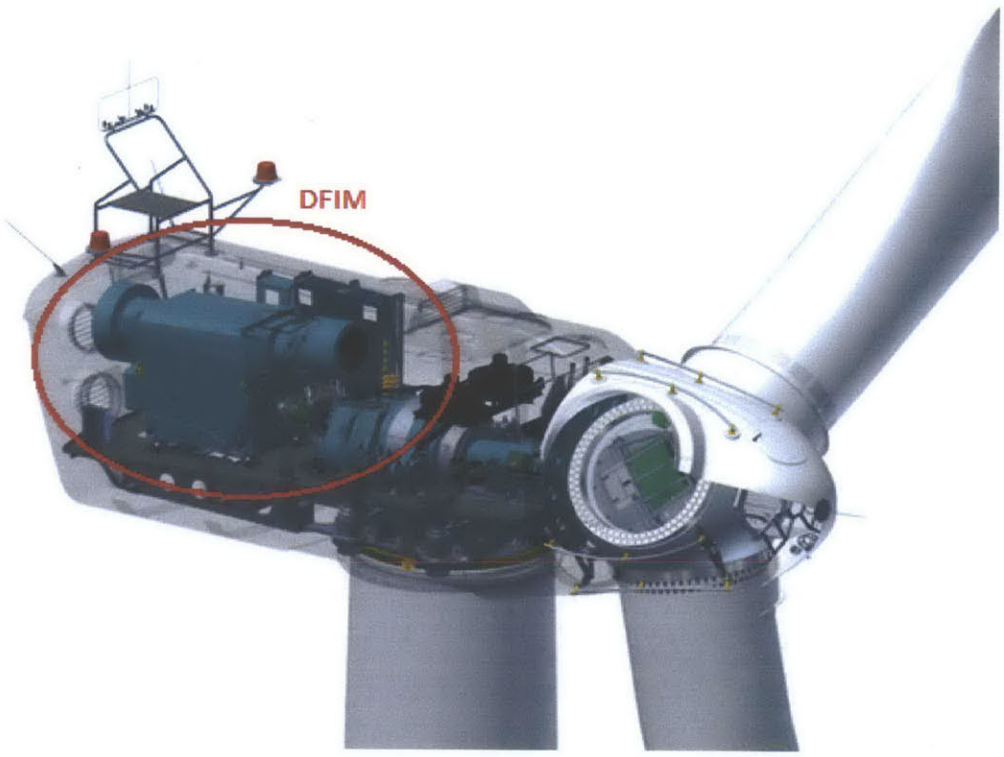

Figure 7. A wind turbine system: S9X cut-way view.

Wind turbines can operate in two modes: fixed speed and variable speed. For the fixed speed case, the induction generator is directly connected to the grid since the speed is almost fixed to the grid frequency, and most certainly not controllable. The rotational energy is not possible to be stored. Therefore, for a fixed speed system the turbulence of the wind will result in power variations, and thus affect the power quality of the grid [2]. For a variable speed wind turbine, the generator is controlled by power electronics converter, which makes it possible to control the rotor speed. In this way the power fluctuations caused by wind variations can be more or less absorbed by changing the rotor speed and thus power variations originating from the wind conversion and the drive train can be reduced. The fixed speed machine imposes reactive power loading on the system and can produce voltage control problem. But more important, it is

inefficient since the coefficient of performance is low then the tip speed ratio is not at optimum. Hence, the power quality impact caused by the wind turbine can be greatly improved.

The variable speed system is discussed throughout the thesis. The block diagram of this system can be described for wound-rotor induction machine

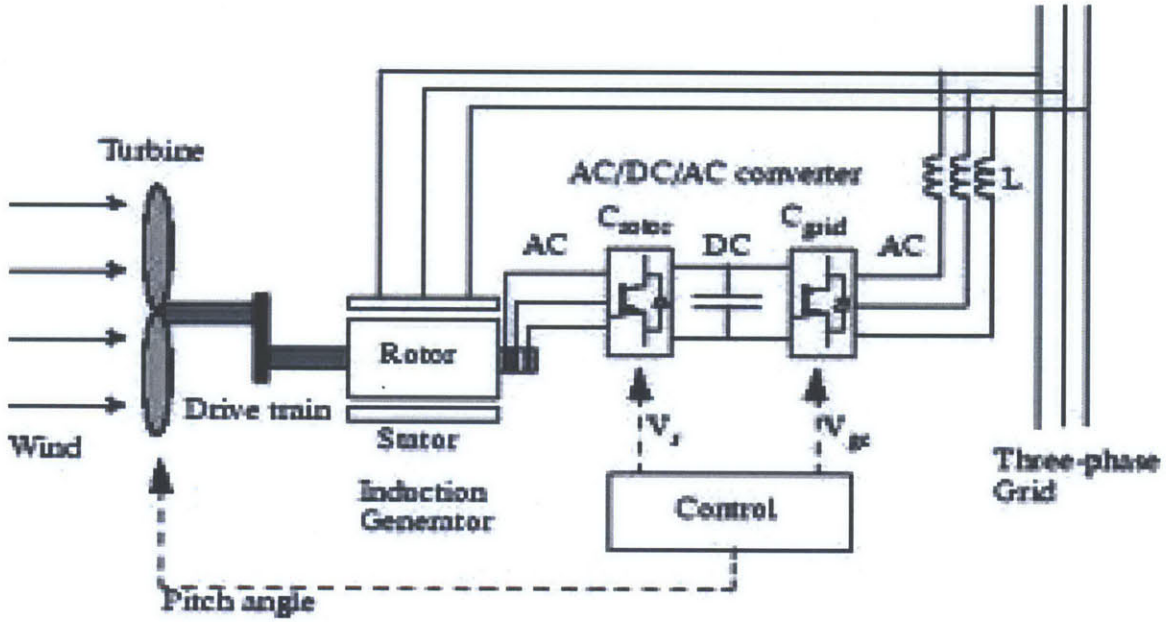

Figure 8. Block Diagram of Wind Turbine System.

This system is complex as the power flows in both directions between the grid and the rotor of the induction machine. Since the wind speed is not fixed in the real world, at its higher value, the machine is operating in the super-synchronous speed and at its lower value, the machine is operating in the sub-synchronous speed. It is challenging to control the power electronics converter to feed the power. A better way to understand this principle is interpreting this power equation derived in the electric machinery class at MIT [3-4]:

$$P_{em}{}^{R} = -sP_{em}{}^{S}$$

If the slip is positive, meaning that the rotor is turning at a speed less than synchronous; if the slip is negative, meaning that the rotor is turning at a speed greater than synchronous.

2.2 Mathematical Modeling

In order to better investigate the characteristic features of DFIM, a detailed mathematic model is analyzed to describe the relationship between flux and inductance and hereafter perform the

simulation. Starting with the equivalent circuit of the DFIM shown in figure 2, the voltage/current equations will be derived.

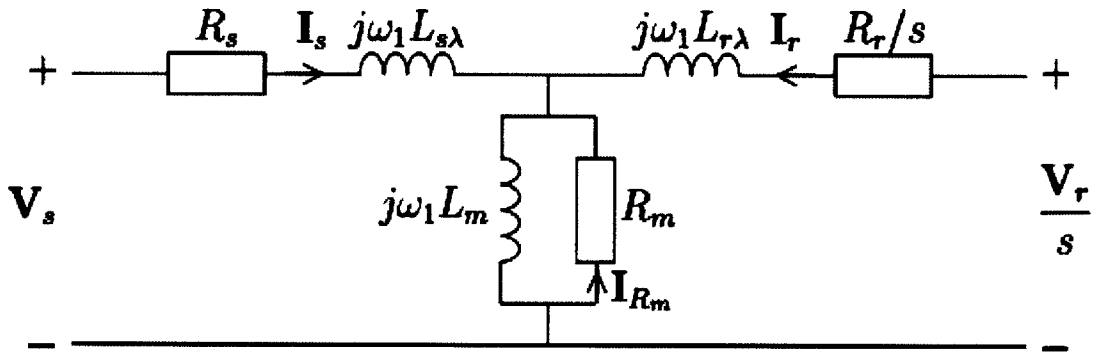

Figure 9. Equivalent circuit of the DFIM.

Applying Park/Clark transformation, the 3-axis coordinate system is transferred into d-q-0 coordinate system, the stator and rotor voltage equations are similar. Here are the stator d-axis and q-axis voltage expressions.

Table 1 Machine Model Variables

p	: Number of pole pairs
Ψ_{sd}	: Stator flux in the direct-axis winding
Ψ_{sq}	: Stator flux in the quadrature-axis winding
Ψ_{rd}	: Rotor flux in the direct-axis damper winding
Ψ_{rq}	: Rotor flux in the quadrature-axis damper winding
r_s	: Stator winding resistances
r_q	: Rotor winding resistance
w	: Stator electrical frequency
w_r	: Rotor electrical frequency
w_m	: Mechanical rotation speed
pw_m	: Electrical rotation speed
δ	: rotor phase angle
L_m	: Mutual inductance between stator and damper windings
L_s, L_r	: Stator inductance, rotor inductance
T_e	: Electromagnetic torque
J	: Rotational inertia constant

The rotor frequency (slip frequency) is

$$w_r = w - pw_m$$

Where slip s is defined by:

$$w_r = sw$$

First, consider the voltages in a frame of reference frame (d-q) that is rotating at synchronous speed with frequency w.

$$v_{sd} = r_s i_{sd} + \frac{\partial \psi_{sd}}{\partial t} - w\psi_{sq}$$

$$v_{sq} = r_s i_{sq} + \frac{\partial \psi_{sq}}{\partial t} + w\psi_{sd}$$

$$v_{rd} = r_r i_{rd} + \frac{\partial \psi_{rd}}{\partial t} - sw\psi_{rq}$$

$$v_{rq} = r_r i_{rq} + \frac{\partial \psi_{rq}}{\partial t} + sw\psi_{rd}$$

Since it is in the synchronous rotating frame, w = w_0, V_{sd}=0, V_{sq} = V. State equations which represents the electrical dynamics of the system can be easily derived.

$$\frac{\partial \psi_{sd}}{\partial t} = v_{sd} + w\psi_{sq} - r_s i_{sd}$$

$$\frac{\partial \psi_{sq}}{\partial t} = v_{sq} - w\psi_{sd} - r_s i_{sq}$$

$$\frac{\partial \psi_{rd}}{\partial t} = v_{rd} + sw\psi_{rq} - r_r i_{rd}$$

$$\frac{\partial \psi_{rq}}{\partial t} = v_{rq} - sw\psi_{rd} - r_r i_{rq}$$

$$\frac{\partial w_m}{\partial t} = \frac{1}{J}(T_e + T_m)$$

$$\frac{\partial \theta_m}{\partial t} = pw_m - w_0$$

The electromagnetic torque is

$$T_e = \frac{3}{2}p(\psi_{sd} i_{sq} - \psi_{sq} i_{sd})$$

After further derivation considering the rotor current equations

$$i_{rd} = \frac{\psi_{rd}}{L_r} - \frac{L_m}{L_r} i_{sd}$$

$$i_{rq} = \frac{\psi_{rq}}{L_r} - \frac{L_m}{L_r} i_{sq}$$

The electromagnetic torque becomes

$$T_e = \frac{3}{2} p \frac{L_m}{L_r} (\psi_{rd} i_{sq} - \psi_{rq} i_{sd})$$

Flux linkage equations are

$$\psi_{sd} = L_s i_{sd} + L_m i_{rd}$$

$$\psi_{sq} = L_s i_{sq} + L_m i_{rq}$$

$$\psi_{rd} = L_r i_{rd} + L_m i_{sd}$$

$$\psi_{rq} = L_r i_{rq} + L_m i_{sq}$$

Hence, current equations is derived by the inverse of inductance matrix

$$\begin{bmatrix} i_{sd} \\ i_{sq} \\ i_{rd} \\ i_{rq} \end{bmatrix} = \begin{bmatrix} \frac{-L_r}{L_m{}^2 - L_r L_s} & 0 & \frac{L_m}{L_m{}^2 - L_r L_s} & 0 \\ 0 & \frac{-L_r}{L_m{}^2 - L_r L_s} & 0 & \frac{L_m}{L_m{}^2 - L_r L_s} \\ \frac{L_m}{L_m{}^2 - L_r L_s} & 0 & \frac{-L_s}{L_m{}^2 - L_r L_s} & 0 \\ 0 & \frac{L_m}{L_m{}^2 - L_r L_s} & 0 & \frac{-L_s}{L_m{}^2 - L_r L_s} \end{bmatrix} \begin{bmatrix} \psi_{sd} \\ \psi_{sq} \\ \psi_{rd} \\ \psi_{rq} \end{bmatrix}$$

Substituting the flux equations into the electromagnetic torque equation to obtain the simplified form of T_e

$$T_e = \frac{3}{2} p L_m (i_{sq} i_{rd} - i_{sd} i_{rq})$$

The mathematical modeling is then fully established for DFIM. These derived equations are organized to make the DFIM model in Matlab simulation environment as shown in figure 10(a).

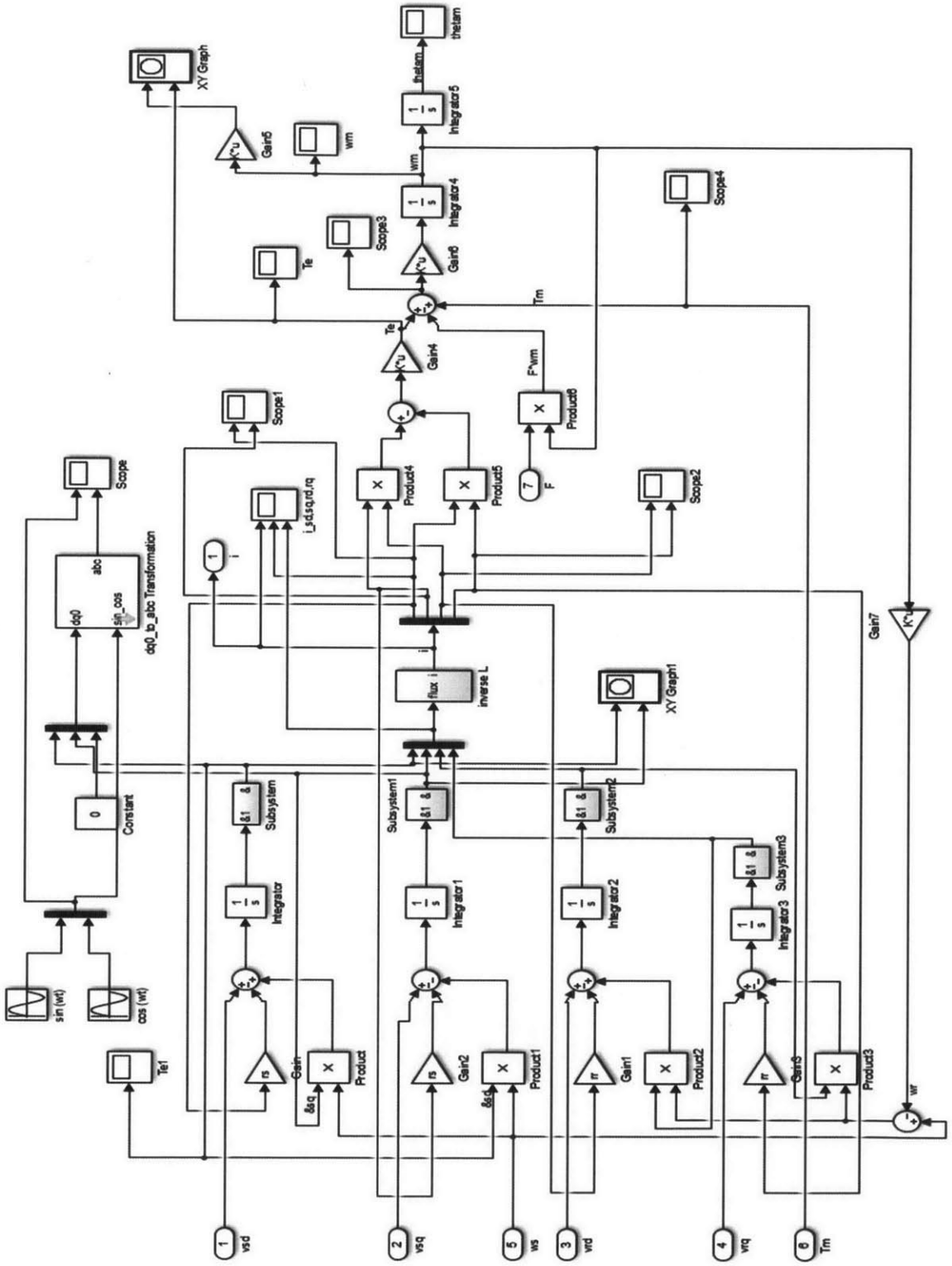

Figure 10(a). Matlab modeling of DFIM.

Since it is relatively time-consuming to run the simulation, a set of parameters is chosen in Table 2 for a four-pole 3HP DFIM in [5] to perform the simulation from transients to steady-state conditions. Since no control scheme is applied, and the rotor is shorted (voltages are zero), thus this machine would behave as a squirrel-cage case. The purpose of this simulation is to verify the functionality of the mathematical model from the previous step. Matlab simulation results are shown in figure 10(b)-10(d).

Table 2 DFIG Simulation Parameters

hp	V_a (V)	T_m (N·m)	Frequency	R_s (Ω)	R_r (Ω)	L_m (H)	L_s (H)	L_r (H)	J (kg·m^2)
3	220	11.9	60	0.435	0.816	0.0693	0.002	0.002	0.089

Transients is designed to have a pulse change of mechanical torque of 11.9 N·m at every 5 seconds for a simulation length of 20s, starting at t =5s.

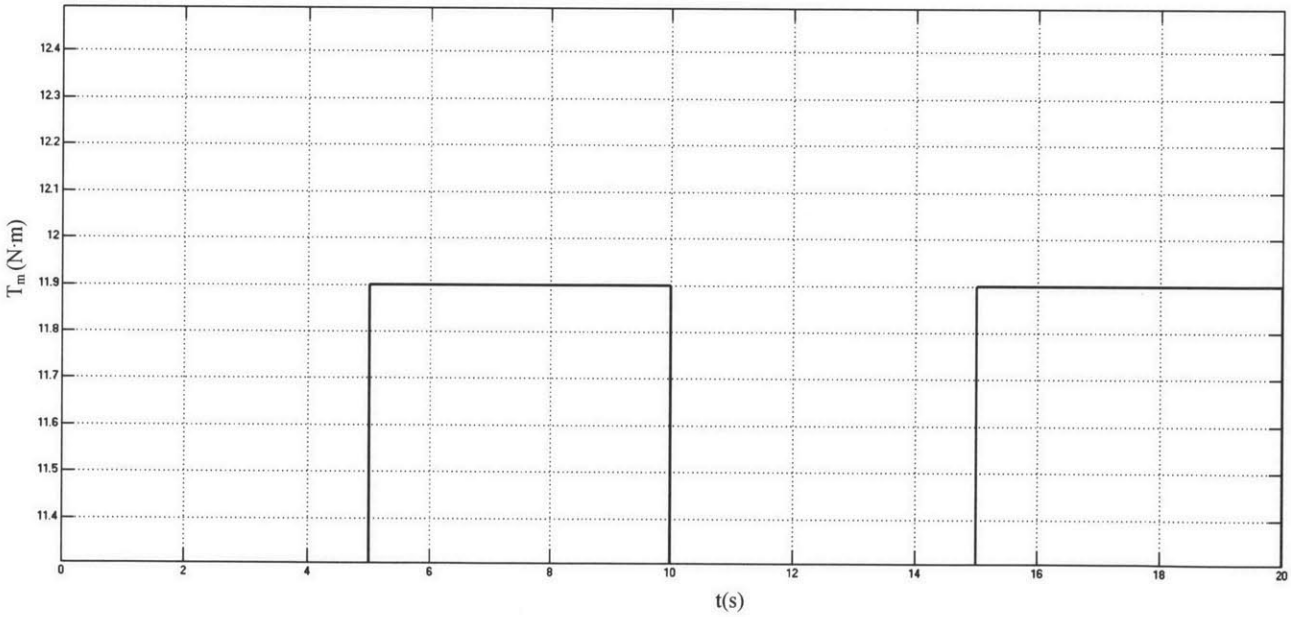

Figure 10(b). Applied mechanical torque.

The instantaneous torque-speed demonstrates a small decayed oscillation at the final operating point, the torque reaches to zero at the steady-state condition.

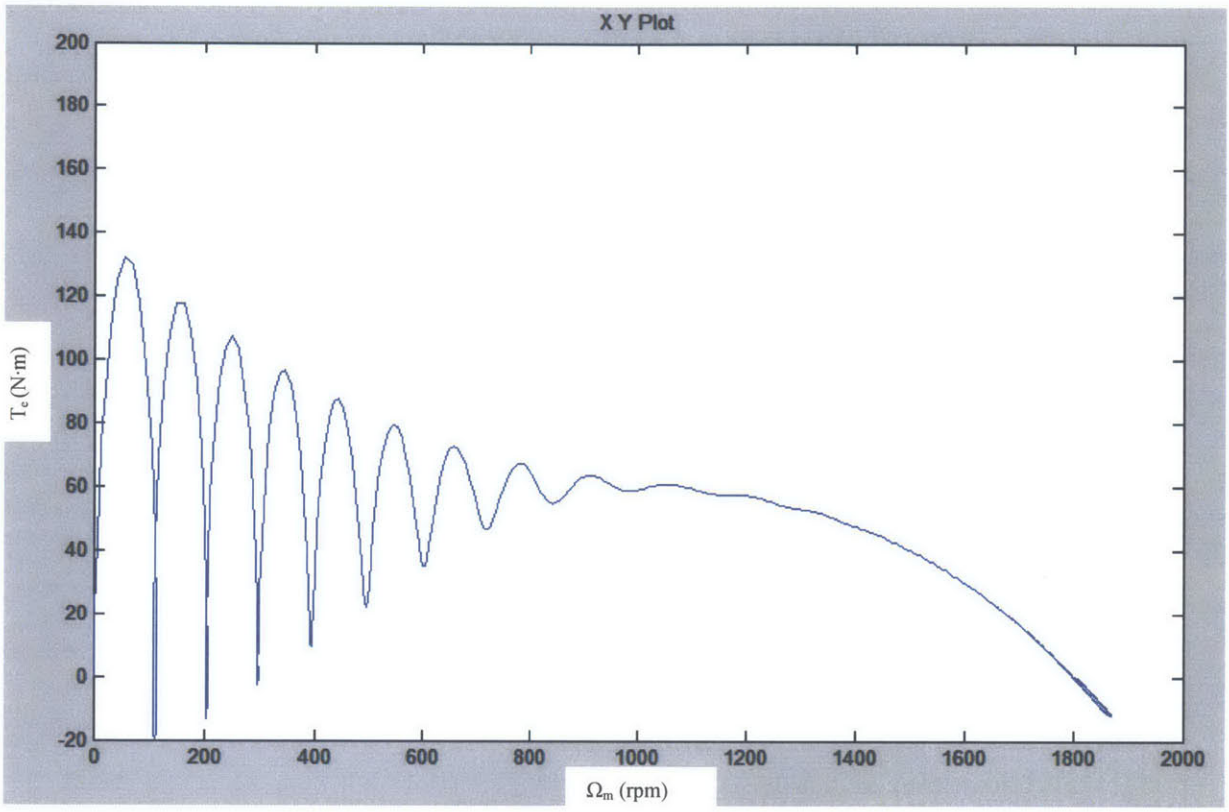

Figure 10(c). Instantaneous torque-speed curve.

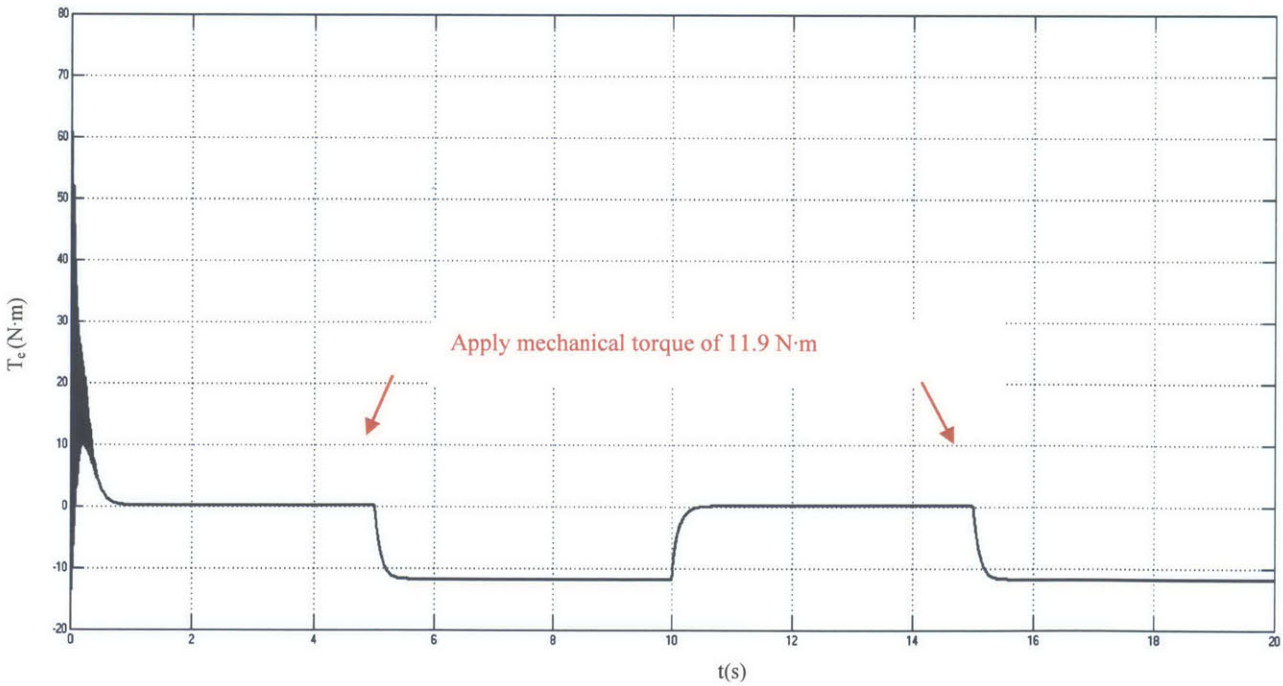

Figure 10(d). Electromagnetic Torque response.

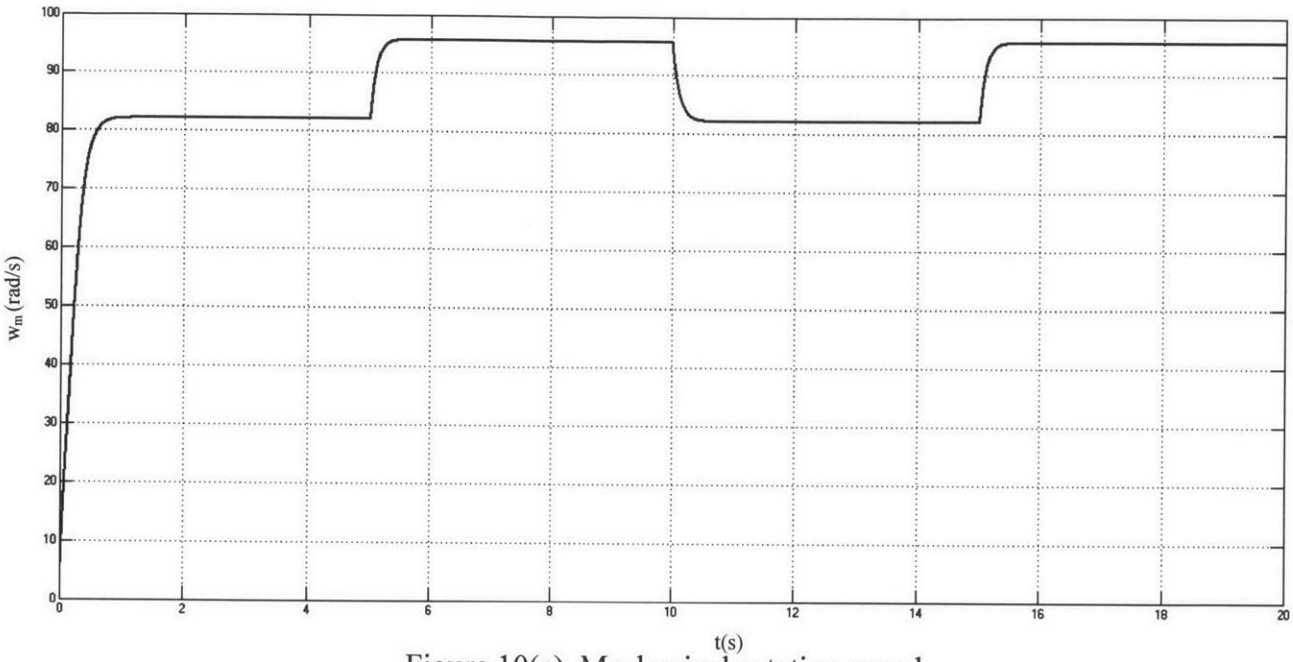

Figure 10(e). Mechanical rotation speed.

The steady-state operation of DFIM is analyzed by its real power and reactive power. The total power of the stator winding is

$$P_s = v_a i_a + v_b i_b + v_c i_c = 3/2(v_{sd} i_{sd} + v_{sq} i_{sq}).$$

Using Matlab tools, its real power and reactive power plots are generated below assuming the mechanical power is constant over a range of the generator speed. The stator output power is equal to the sum of the rotor input power and mechanical power.

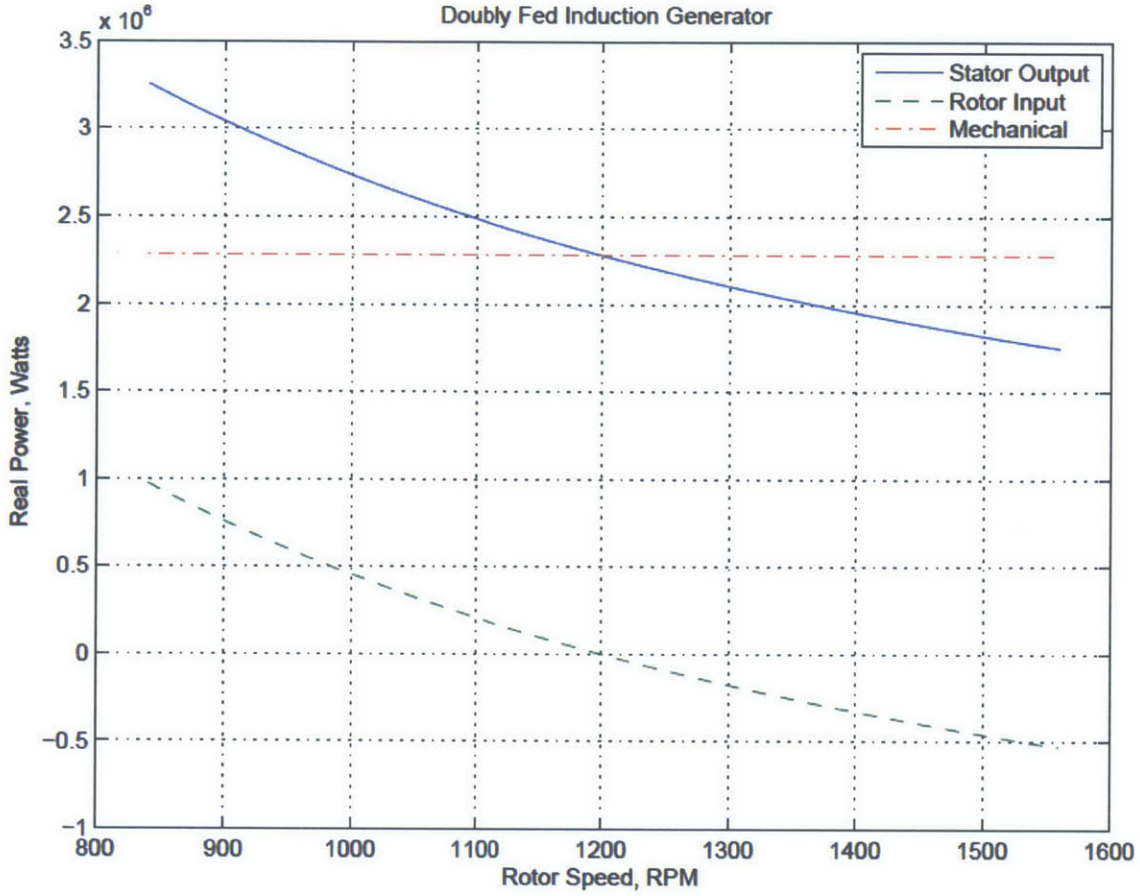

(a) Real power of DFIM

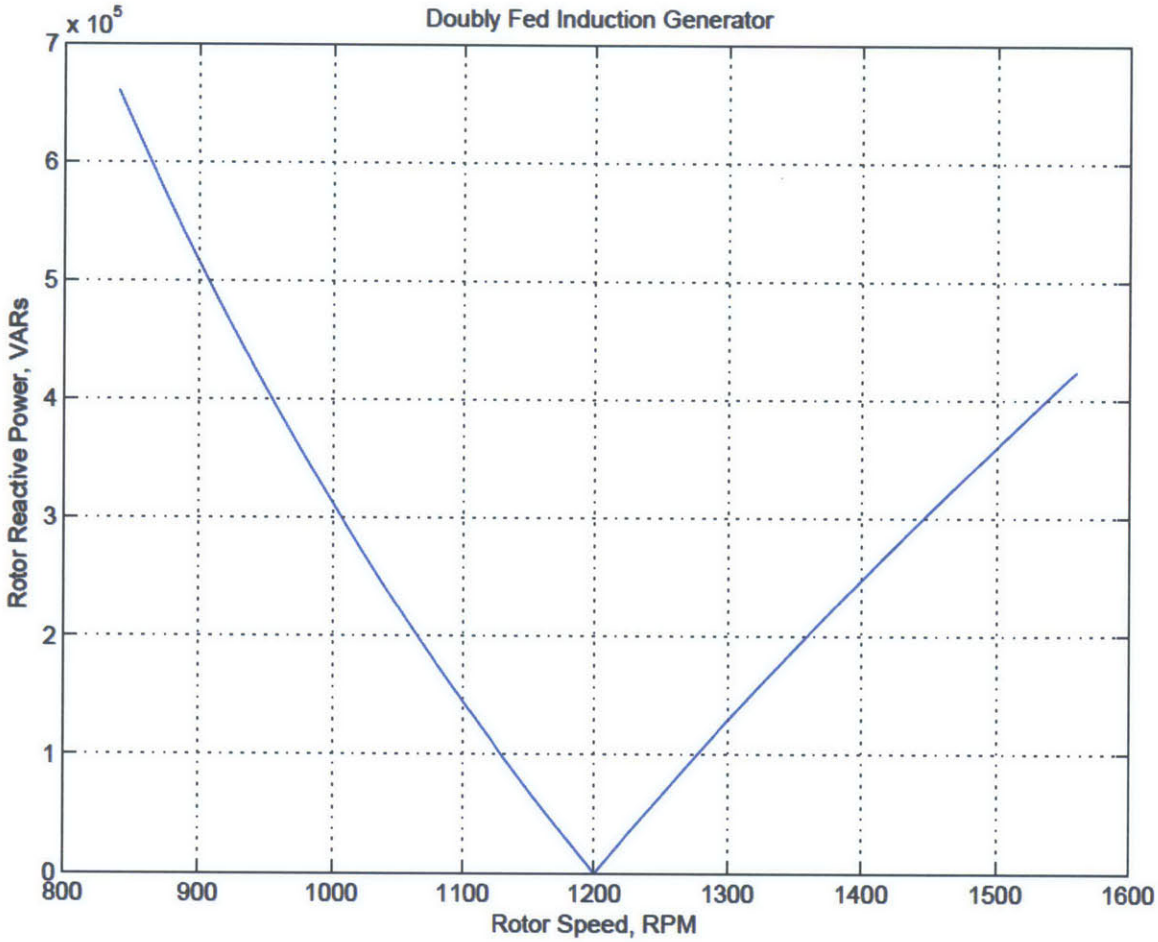

(b) Reactive power of DFIM

Figure 11. Operation of DFIM.

This operation is based on the assumption that the converter interacts with the machine stator terminal at unity power factor, indicating zero reactive power drawn or supplied by the right-hand end of the converter. In this application, rotor real power is stator real power times slip; reactive power is supplied by and controlled by the rotor side converter.

In terms of the power electronics system, the DC/AC inverter on the grid side is connected to a third-order L-C-L filter as shown in figure 12. Its role in voltage-source control based grid converter is twofold. On the one side, the grid filter should have a dominant inductive behavior to guarantee the proper operation of the voltage source converter if connected to a utility grid which is a voltage source type system. On the other side, VSC-based grid converters generate PWM carrier and side-band voltage harmonics, causing the current flowing into the grid, eventually

disturb other sensitive loads. At a system level, standards and grid codes recommend compliance with limitations that are very stringent for frequencies above a certain threshold. Hence a high-order low-pass L-C-L filter is preferred, which provide 60dB/decade attenuation, in such way the two mentioned requirements are satisfied.

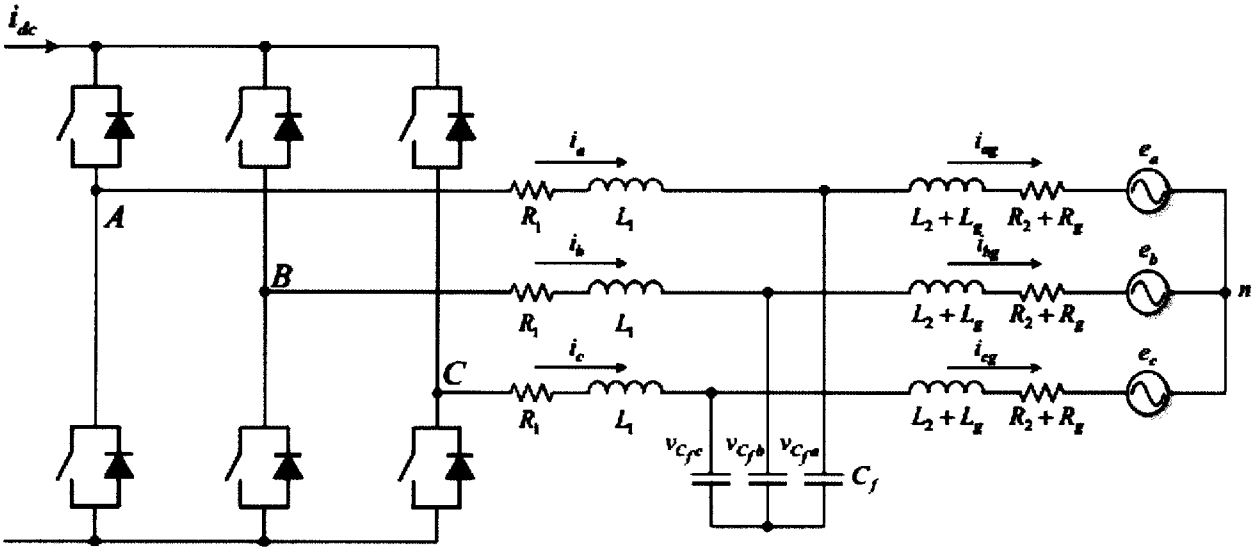

Figure 12 (a). DC/AC Inverter on the grid side with L-C-L filter without damping circuit.

The mathematical modeling of the L-C-L filter is organized as follow, the damping circuit is not considered at this case for the simplicity.

If the switching function of the top switch in each bridge is defined as p(t), p(t) is equal to 1 when the upper switch is closed and 0 when the lower switch is closed.

$$\bar{p}(t) = \frac{2}{3}(p_a(t) + p_b(t)e^{j2\pi/3} + p_c(t)e^{j-2\pi/3})$$

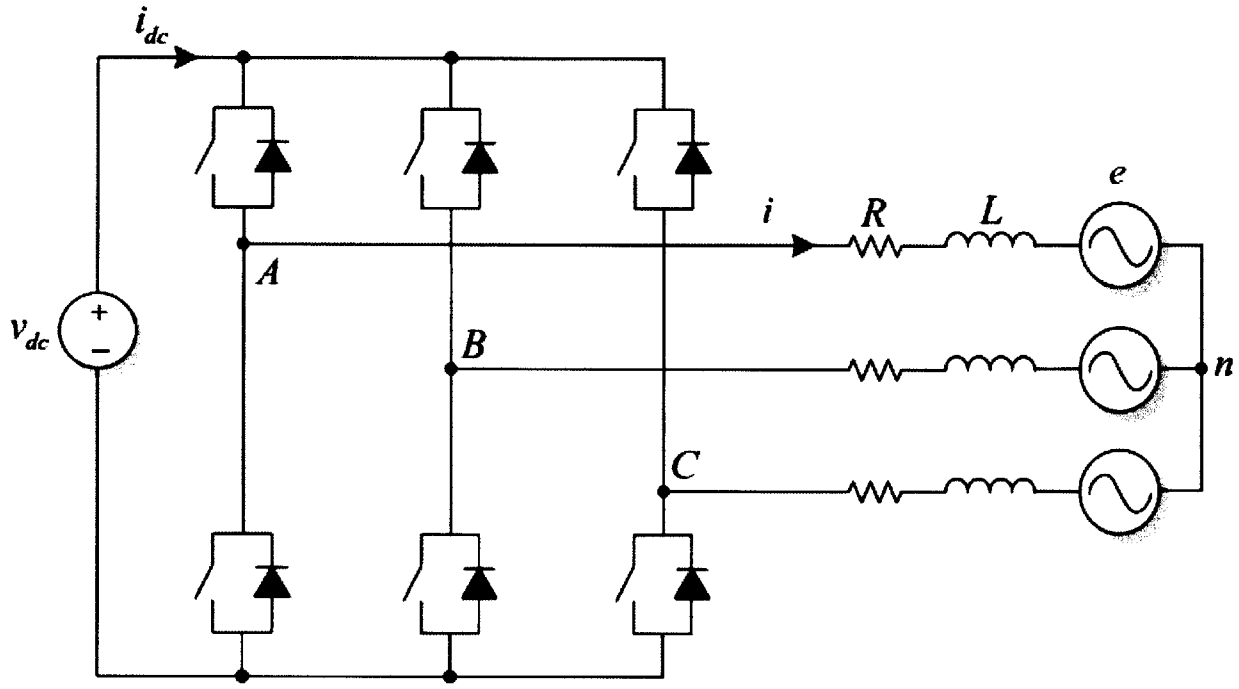

Figure 12(b). DC/AC Inverter on the grid side with only L-filter.

Consider this simplified system first, in which case the inverter is only connected to a L filter, hence the AC-side voltage of the inverter is

$$\bar{v}(t) = \bar{p}(t)v_{dc}(t)$$

The state-space equation of this is

$$\frac{d\bar{\imath}(t)}{dt} = \frac{1}{L}[-R\bar{\imath}(t) - \bar{e}(t) + \bar{p}(t)v_{dc}(t)]$$

where $\bar{\imath}(t)$ is the inverter current, $\bar{e}(t)$ is the input line voltage.

Apply the park transformation to derive p_d and p_q, and consider the angular speed w, then the electrical equations in d-q-0 frame can be established in this way.

$$\frac{di_d(t)}{dt} - wi_q(t) = \frac{1}{L}[-Ri_d(t) - e_d(t) + p_d(t)v_{dc}(t)]$$

$$\frac{di_q(t)}{dt} + wi_d(t) = \frac{1}{L}[-Ri_q(t) - e_q(t) + p_q(t)v_{dc}(t)]$$

Further, consider the L-C-L filter case (without the damping circuit), the mathematical formulation of this circuit is derived below.

$$\frac{d}{dt}\begin{bmatrix} i_d \\ i_q \\ v_{Cfd} \\ v_{Cfq} \\ i_{gd} \\ i_{gq} \end{bmatrix} = \begin{bmatrix} -\frac{R_1}{L_1} & \omega & -\frac{1}{L_1} & 0 & 0 & 0 \\ -\omega & -\frac{R_1}{L_1} & 0 & -\frac{1}{L_1} & 0 & 0 \\ \frac{1}{C_f} & 0 & 0 & \omega & -\frac{1}{C_f} & 0 \\ 0 & \frac{1}{C_f} & -\omega & 0 & 0 & -\frac{1}{C_f} \\ 0 & 0 & \frac{1}{(L_2+L_g)} & 0 & -\frac{(R_2+R_g)}{(L_2+L_g)} & \omega \\ 0 & 0 & 0 & \frac{1}{(L_2+L_g)} & -\omega & -\frac{(R_2+R_g)}{(L_2+L_g)} \end{bmatrix} \begin{bmatrix} i_d \\ i_q \\ v_{Cfd} \\ v_{Cfq} \\ i_{gd} \\ i_{gq} \end{bmatrix}$$

$$+ \begin{bmatrix} 0 & 0 \\ 0 & 0 \\ 0 & 0 \\ 0 & 0 \\ -\frac{1}{L_1} & 0 \\ 0 & -\frac{1}{L_1} \end{bmatrix} \begin{bmatrix} e_d \\ e_q \end{bmatrix} + \begin{bmatrix} \frac{v_{dc}}{(L_2+L_g)} & 0 \\ 0 & \frac{v_{dc}}{(L_2+L_g)} \\ 0 & 0 \\ 0 & 0 \\ 0 & 0 \\ 0 & 0 \end{bmatrix} \begin{bmatrix} p_d \\ p_q \end{bmatrix}$$

It is always necessary to consider the damping circuit for the L-C-L filter due to the resonance problem; thus a damping circuit which use a damping resistor in series with a DC blocking capacitor is designed in chapter 5.

Chapter 3 CONTROL ALGORITHM

3.1 Space Vector Modulation

Park Transformation

Park transformation is a mathematical transformation which converts traditional a-b-c phase coordination system to the direct axis and quadrature-axis coordination system. This can be represented in a straightforward fashion in terms of electrical angel between the rotor direct axis and stator phase-a axis.

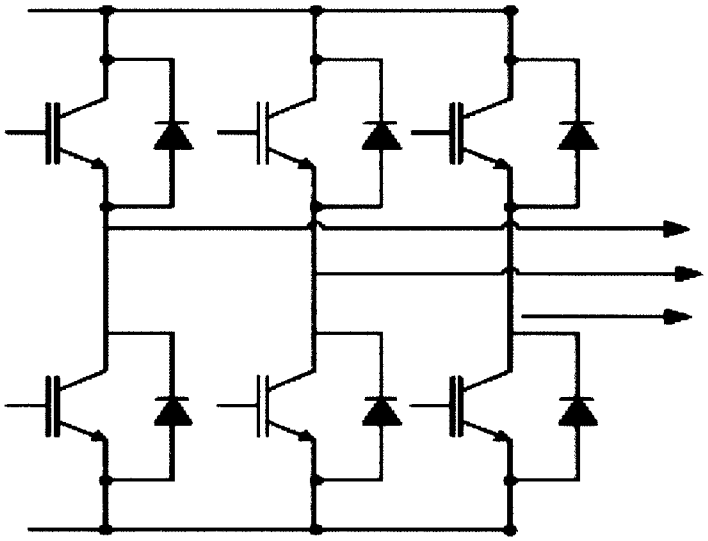

Figure 13. Three-Phase Six-Switch Bridge.

For a better understanding, here I am using an example of the PFC AC/DC rectifier control using SVPWM [6]. From the analysis of three-phase six-switch topology as shown in figure 14, the source voltages and currents need to be converted into d-q frame by the application of park transformation (1).

$$\begin{bmatrix} f_d^r \\ f_q^r \\ f_0^r \end{bmatrix} = \frac{2}{3} \begin{bmatrix} \cos\theta_r & \cos(\theta_r - \frac{2\pi}{3}) & \cos(\theta_r + \frac{2\pi}{3}) \\ \sin\theta_r & \sin(\theta_r - \frac{2\pi}{3}) & \sin(\theta_r + \frac{2\pi}{3}) \\ \frac{1}{2} & \frac{1}{2} & \frac{1}{2} \end{bmatrix} \begin{bmatrix} f_a \\ f_b \\ f_c \end{bmatrix} \quad (1)$$

Here f represents the phase voltage and current of the grid. Through eqn (1), the grid voltage and current could be successfully transformed into $V_{d/q}$ and $i_{d/q}$. In order to obtain reference current $I_{d,ref}$ (note for power factor equal to 1, the $I_{d,ref}$=0) and error voltage $U_{d,err}$ and $U_{q,err}$, three PI voltage and current controllers are applied as shown in figure 14.

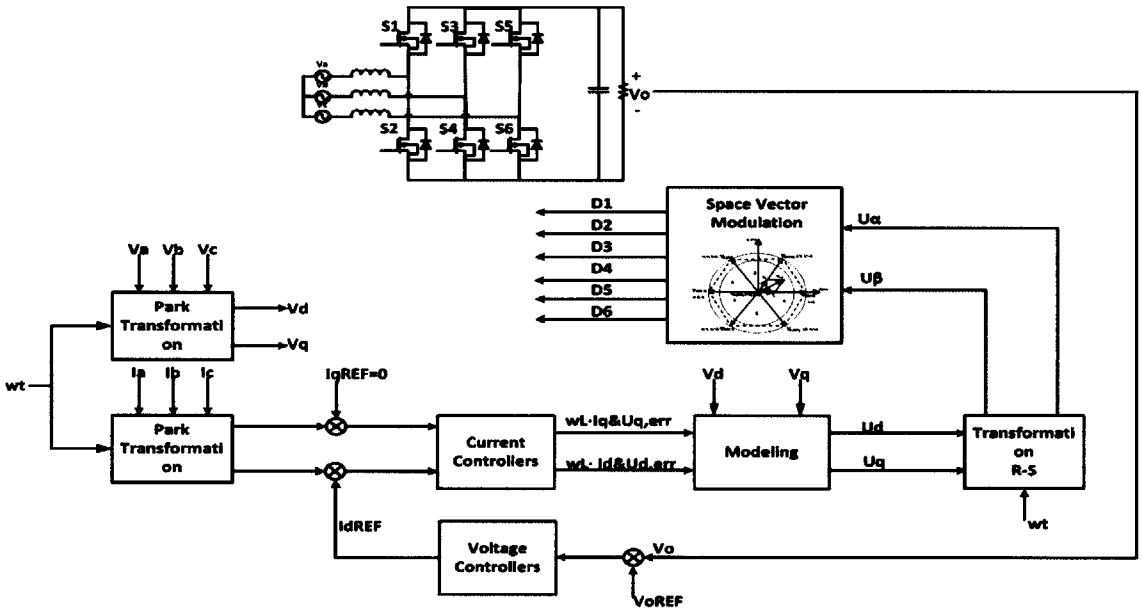

Figure 14. Control structure of a PFC AC/DC rectifier.

Therefore the output voltage the three-phase full bridge is

$$\begin{aligned} U_d &= V_d + \omega L \cdot i_q - U_{d,err} \\ U_q &= V_q - \omega L \cdot i_d - U_{q,err} \end{aligned} \quad (2)$$

Vector Control

Next step is the transformation from the rotating frame (d-q-0) is transformed to stationary reference frame (α-β-0)

$$\begin{bmatrix} f_\alpha \\ f_\beta \\ f_0 \end{bmatrix} = \begin{bmatrix} 0 & \cos\ \theta_r & -\sin\ \theta_r \\ 0 & \sin\ \theta_r & \cos\ \theta_r \\ 1 & 0 & 0 \end{bmatrix} \begin{bmatrix} f_d \\ f_q \\ f_0 \end{bmatrix} \tag{3}$$

Therefore

$$\begin{aligned} U_\alpha &= U_d \cdot \cos\theta_r - U_q \cdot \sin\theta_r \\ U_\beta &= U_d \cdot \sin\theta_r + U_q \cdot \cos\theta_r \end{aligned} \tag{4}$$

Hence

$$\begin{aligned} V_{ref} &= \sqrt{U_\alpha{}^2 + U_\beta{}^2} \\ \alpha &= \arctan\frac{U_\beta}{U_\alpha} \end{aligned} \tag{5}$$

where V_{ref} could be realized by the six non-zero vector and two zero vectors shown in figure 13.

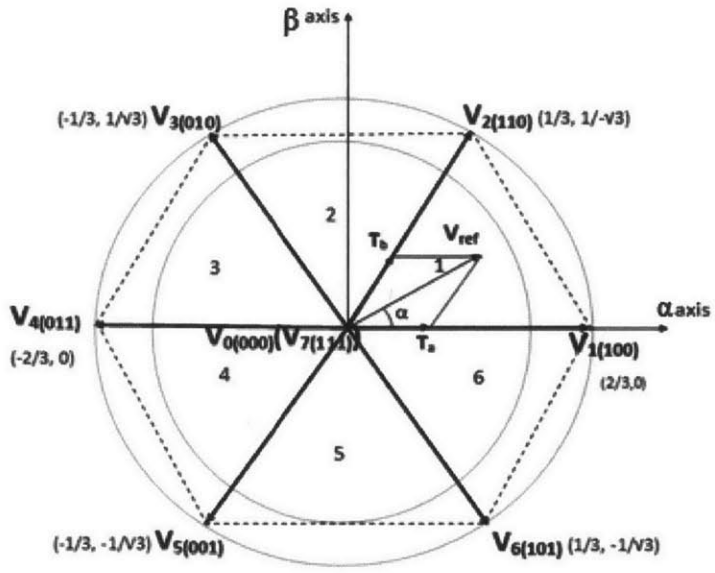

Figure 15. Space vector coordinates.

For example, the vector V_{ref} in figure 15 is implemented as

$$\overrightarrow{V_{ref}} = V_1 \cdot \frac{T_a}{T_s} + V_2 \cdot \frac{T_b}{T_s} + (V_o or V_7) \cdot \frac{T_0}{T_S} \tag{6}$$

where T_s is the period of a switching cycle.

$$\begin{aligned} V_1 &= V_2 = \frac{2}{3} V_{dc} \\ T_a &= \frac{V_a}{V_1} \cdot T_s \\ T_b &= \frac{V_b}{V_2} \cdot T_s \\ T_0 &= T_s \cdot (1 - t_a - t_b) \end{aligned} \tag{7}$$

Therefore the duty-cycle of the V_a and V_b is

$$D_a = \frac{T_a}{T_s} = \frac{V_{ref}}{\frac{2}{3}V_{dc}}\left[\cos\alpha - \frac{1}{\sqrt{3}}\sin\alpha\right] \tag{8}$$

$$D_b = \frac{T_b}{T_s} = \frac{V_{ref}}{\frac{2}{3}V_{dc}} \cdot \frac{2}{\sqrt{3}} \cdot \sin\alpha$$

When implementing the voltage vectors, different sequence could be selected, i.e., the symmetric SVPWM, asymmetric SVPWM techniques and traditional control, as shown in Table 3, $V_0 - V_7$ are referred to the corresponding states in Space Vector coordinates of figure 15.

Table 3 SVPWM Drive Signals Comparison

SVPWM Control Algorithm	Drive Signals
Traditional	$V_0V_1V_2\ V_7V_2V_1V_0$
Asymmetric	$V_0V_1V_2V_2V_1V_0/V_7V_2V_1V_1V_2V_7$
Symmetric	$V_0V_1V_2V_7V_2V_1V_0$

Accordingly, drive signals for symmetric SVPWM is shown below in figure 16.

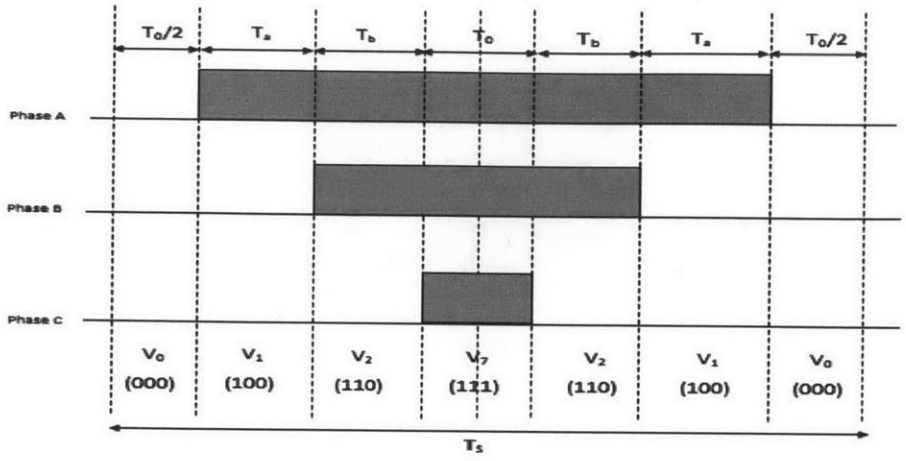

Figure 16. Drive Signals for symmetric SVPWM.

Seen from figure 17(a)-(c), duty cycles of symmetric SVPWM can reach to values of both zero and one hundred percent, duty cycles of asymmetric SVPWM can reach a value of either zero or one hundred percent; however duty cycles of traditional symmetric never reach to a value of zero and one hundred percent. This means, for the symmetric control, there is always 1/6 of the period when the switch is forever on and another 1/6 when the switch is forever off. So it is expected to have less switching loss. But it might have the conflict with the minimum pulse width, which should be addressed in the real applications.

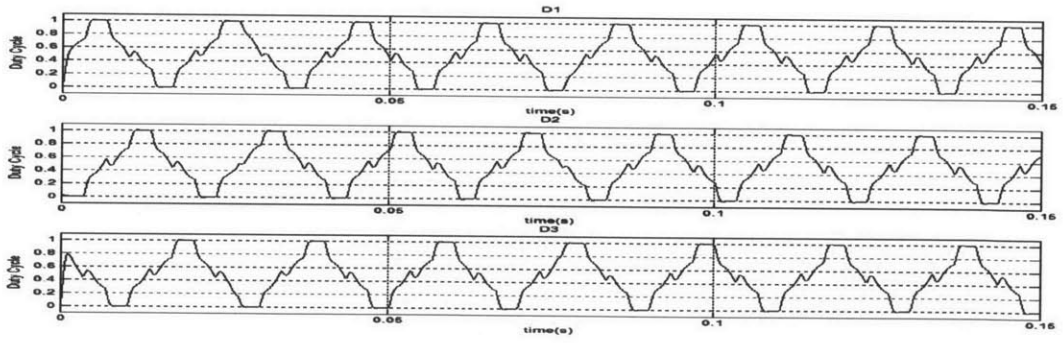

Figure 17(a). Duty Cycle for upper switches under symmetric SVPWM.

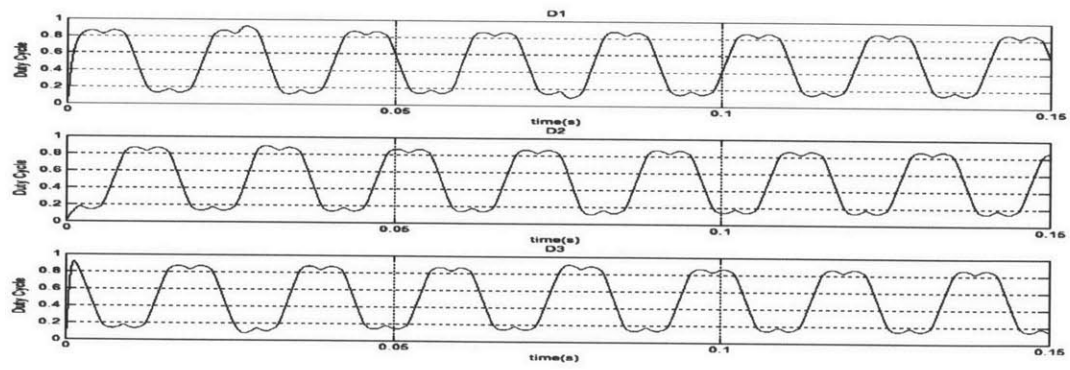

Figure 17(b). Duty Cycle for upper switches under traditional SVPWM.

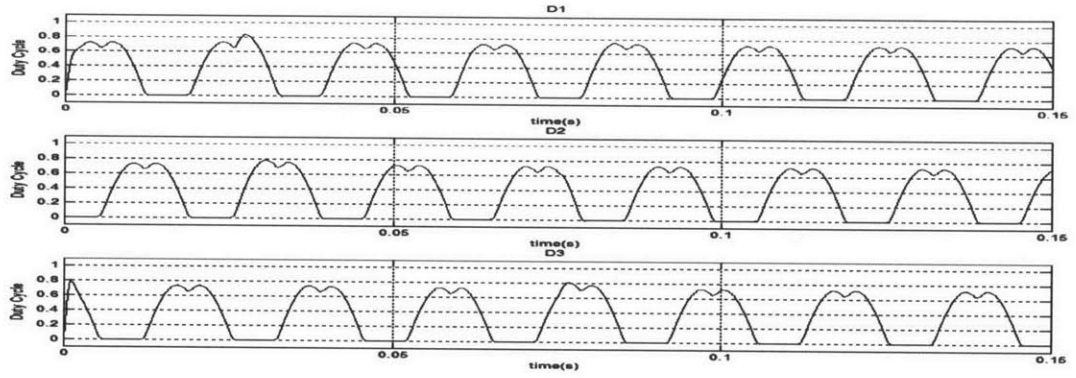

Figure 17(c). Duty Cycle for upper switches under asymmetric SVPWM.

3.2 Field Oriented Control

Field Oriented Control is widely used in DFIM. It is applied to control the rotor current by the means of vector control. Generally speaking, stator-flux orientation and air-gap flux orientation are the two approaches. Rotor-flux and stator-flux are two common FOC methods. A comparison of both schemes at steady state and during transients were presented in [8]. Noteworthy is that both schemes have got nearly the same dynamics; the resulting differences are insignificant. The RFOC has some negligible disadvantages in view of larger coupling of the both reference frame axes.

3.3 Direct Torque Control

The Direct Torque Control (DTC) technique was proposed by I. Takahashi and T. Noguchi in 1986 [9]. Direct Torque Control is an alternative to the classical Field Orientated Control widely used in drive control. The distinguished features are the reduction of decoupling vectors and the rotation coordinate transform. Instead, the control system obtains the instantaneous flux and torques by space vector based on the measured voltages and currents.

The objectives of DTC are the control of the reactive power interchanged between the generator and the grid, and the control of the power drawn from the wind turbine in order to track the wind turbine optimum operation point. However, this system suffers from variable switching frequency and inherent torque ripple. Thus SVM technique is applied to DTC to overcome the mentioned drawbacks.

The DTC-SVM technique estimates the rotor flux and torque. These equations have been derived in the mathematical modeling part of Chapter 2. The coordination frame needs to be transformed from d-q-0 rotating frame to stationary α-β-0.

First, Rotor flux is estimated by the measured voltages and currents from the rotor of DFIM.

$$\psi_{r\alpha} = L_r i_{r\alpha} + L_m i_{s\alpha}$$

$$\psi_{r\beta} = L_r i_{r\beta} + L_m i_{s\beta}$$

Then, electromagnetic torque is estimated from

$$T_e = \frac{3}{2} p(\psi_{r\alpha} i_{r\beta} - \psi_{r\beta} i_{r\alpha})$$

Rotor flux angle is calculated from

$$\theta_r = arctan \frac{\psi_{r\alpha}}{\psi_{r\beta}}$$

Given the torque reference value, the torque difference is applied to PI controller to obtain the load angle $\Delta\delta$ between the rotor and stator fluxes.

Then the rotor flux is calculated from the load angle $\Delta\delta$ and rotor flux reference ψ_r^{ref}, which is shown in the diagram below. From the rotor flux difference between this calculated rotor flux and the estimated rotor flux, space vector signals of the switches are further determined.

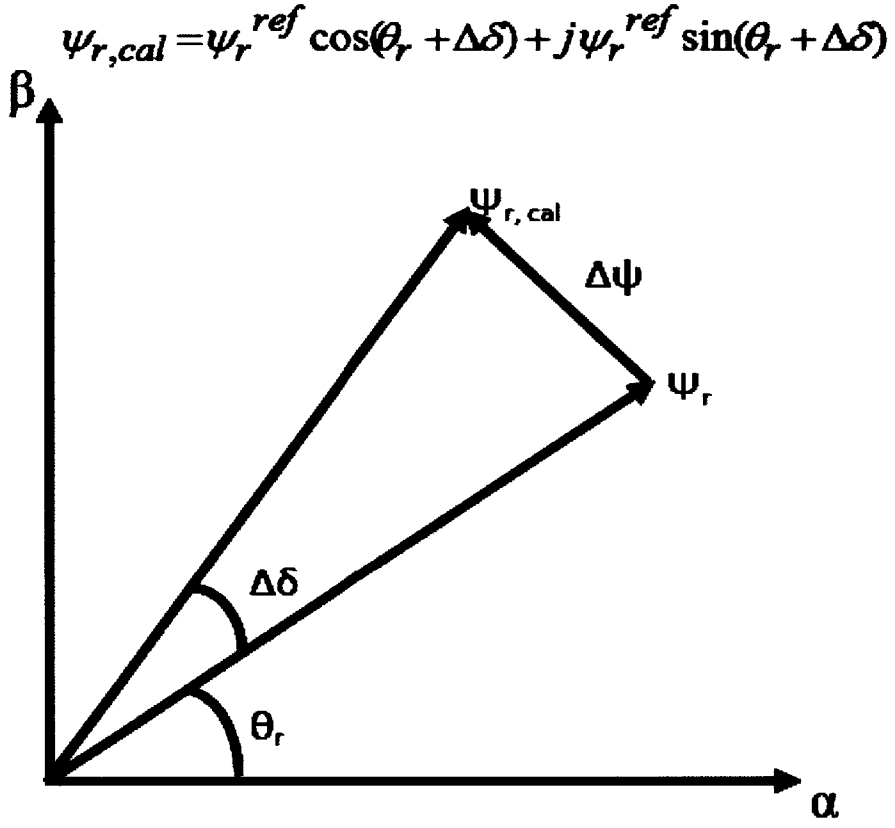

Figure 18 (a). Rotor flux diagram.

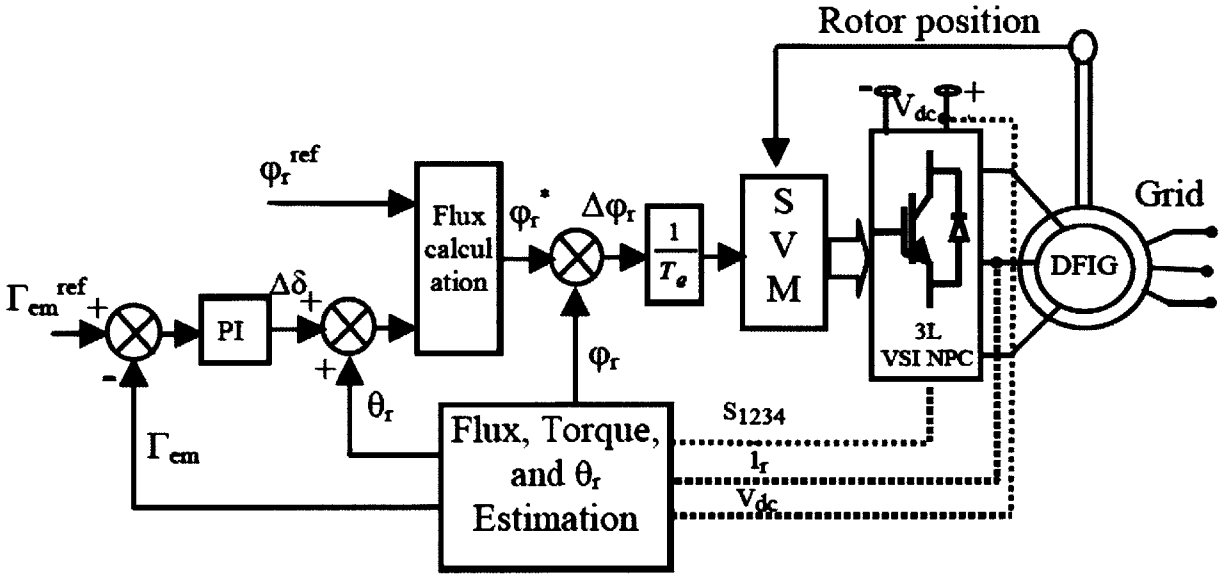

Figure 18(b). DTC-SVM Control Scheme.

3.4 Inverter Current Control

For the inverter, a current control is applied as shown in figure 19. Space Vector Modulation is used to generate the desired PWM output. As discussed earlier, this algorithm represents the eight inverter states including 6 state vectors and 2 null vectors. Basically this method can be regarded as a single vector rotating counter-clockwise around the origin. The time taken for the vector to compute one revolution is equal to the period of the output waveform. By setting this period properly we controlled the desired output frequency within a resolution of 0.1Hz. An interesting challenge in using the SVM algorithm is the tradeoff between the output frequency resolution and the number of elements in the look-up table as the look-up table size is limited by the memory of the micro-controller if high resolution is desired. Hence time pre-scaling parameters in the micro-controller is used to achieve high resolution without the need for massive look-up tables.

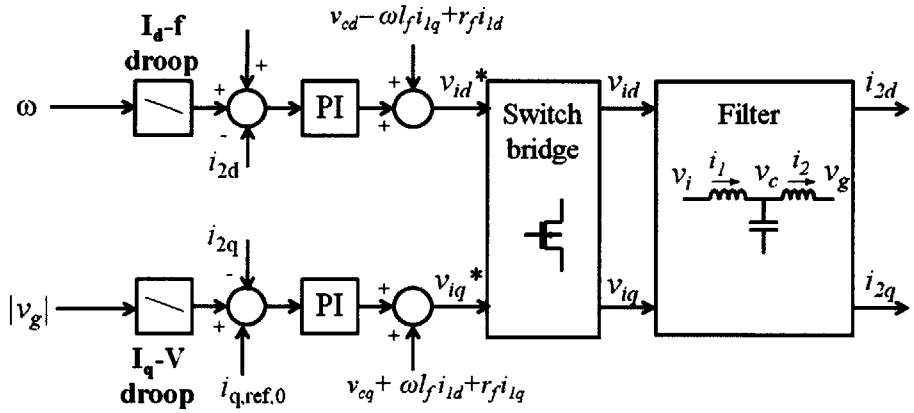

Figure 19. DC/AC Inverter Control Scheme.

Chapter 4 HARDWARE IMPLEMENTATION

In order to conduct the experiment for DGIMs, the author designed and constructed a 2.5kW DC/AC inverter and a L-C-L grid-connected filter. The inverter system for the Microgrid consists of a 3 phase H-bridge converter with an LCL filter at the output. The board was designed to withstand currents up to 50 Amps so that short circuit tests can be performed.

The DC/AC inverter is designed to have a dimension of 9inch (length) by 5.36inch (width) and the grid filter board is 12.38inch (length) by 8.61inch (length).

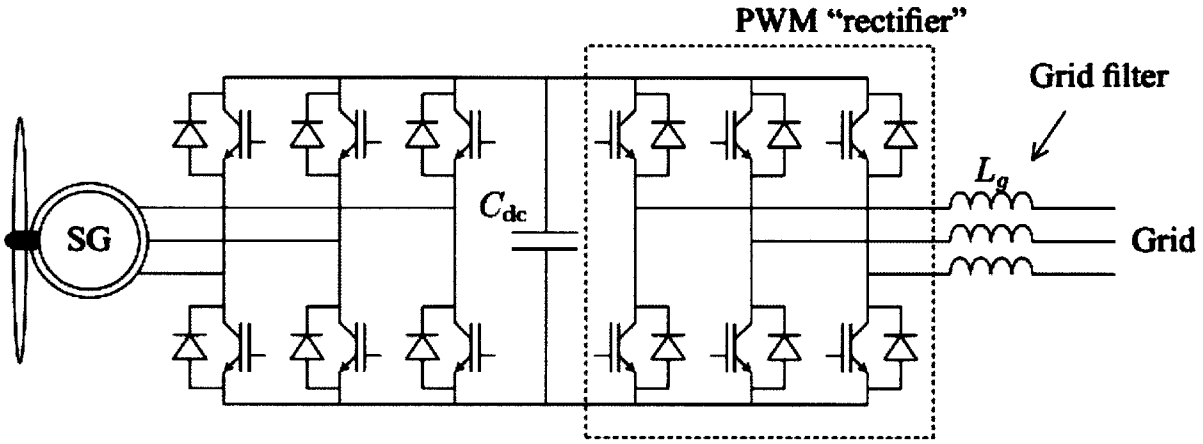

Figure 20. Power Electronics of DFIM system.

4.1 2.5kW inverter construction

The author updated the 2.5kW inverter from the previous design to resolve the issues with the filter circuit as discussed below.

The figure below shows the inverter's output voltage for phase A in the presence of little load. This output was filtered using an L-C-L filter. The FFT for the waveform is also included below. The Total Harmonic Distortion (THD) was calculated to be 0.28% during low load operation.

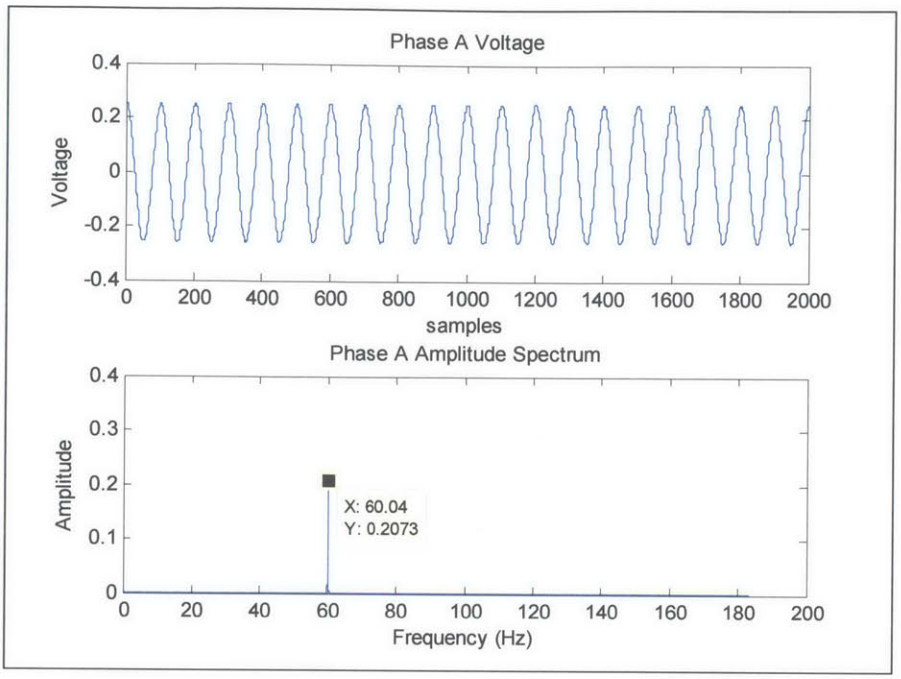

Figure 21. Inverter output after high pass filtering.

The above experiment was carried out using a previous version of the circuit. Because of issues with the inverter and filter circuit, the printed circuit board was redesigned and updated inverter board has been constructed and well tested.

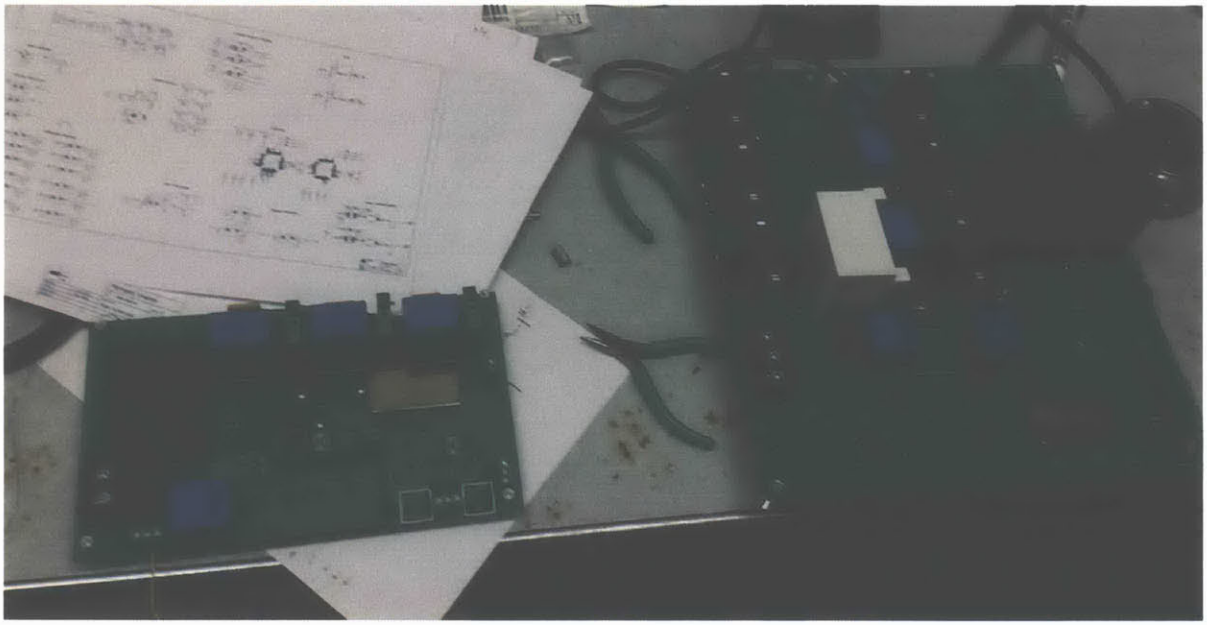

Figure 22(a). Inverter board updates (previous and current versions).

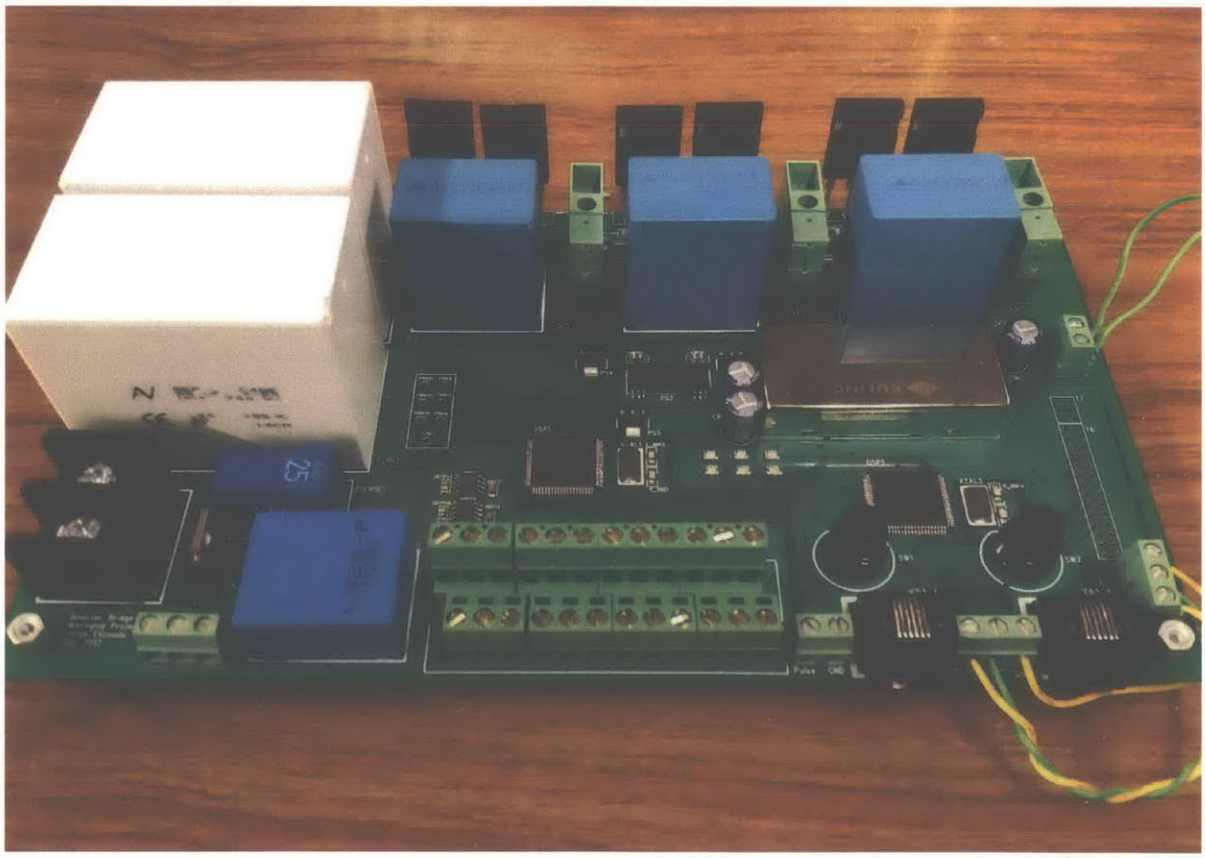

Figure 22(b). Updated Inverter Board.

4.2 L-C-L grid filter design and construction

The current design of the grid filter involves a three-phase L-C-L filter which attenuates the high frequency components from the inverter, providing the clean signals to the grid. Its schematic is shown below, and please note that values are still tentative: to be updated during the test session. Grid filter is needed to be designed after the converter output. As for the noise attenuation, the author designed a three-phase L-C-L filter after the convert output to provide clean signals to the grid. Basic idea is to calculate the values of inductors, capacitors, and damping resistors, and simulate these values in the noise environment, then the author perform inductor design on the selected cores.

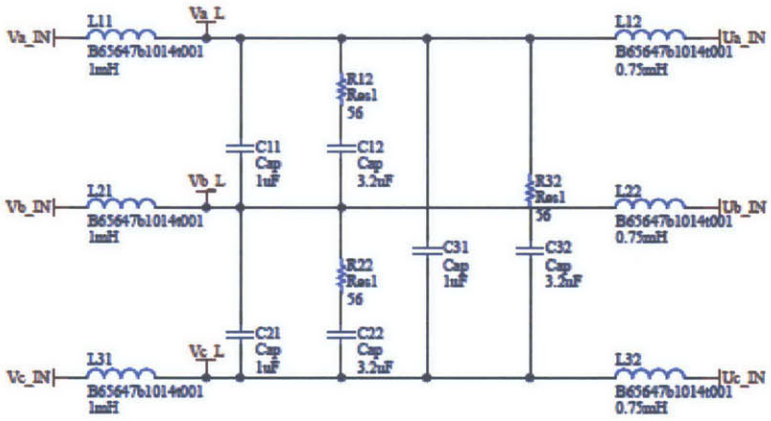

Figure 23. L-C-L filter circuit.

L-C-L filter design is as follows:

1. Ripple Analysis and converter-side inductor choice

$$\Delta I = \frac{V_{dc}}{L_1 f}$$

Where ΔI is the ripple current, V_{dc} is the DC link capacitor voltage 250V, f is the switching frequency of the inverter, L_1 is the inductor on the convert-side.

2. Harmonic attenuation of the filter, resonance frequency value, and damping circuit design

The purpose of damping circuit is to prevent the infinite value of the iy/ix transfer function at its resonant frequency. The damping circuit is a damping resistor R_d in series with a large dc blocking capacitor C_d

3.

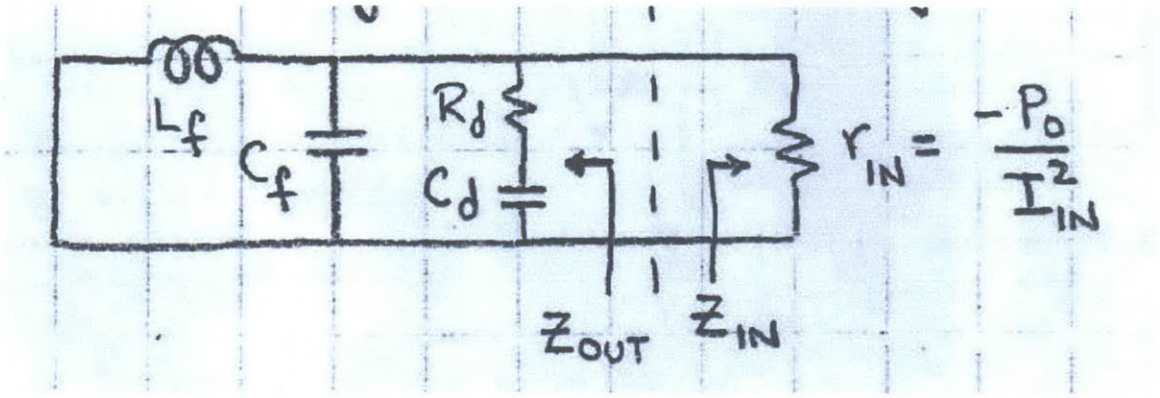

(a) Damping circuit and output resistance

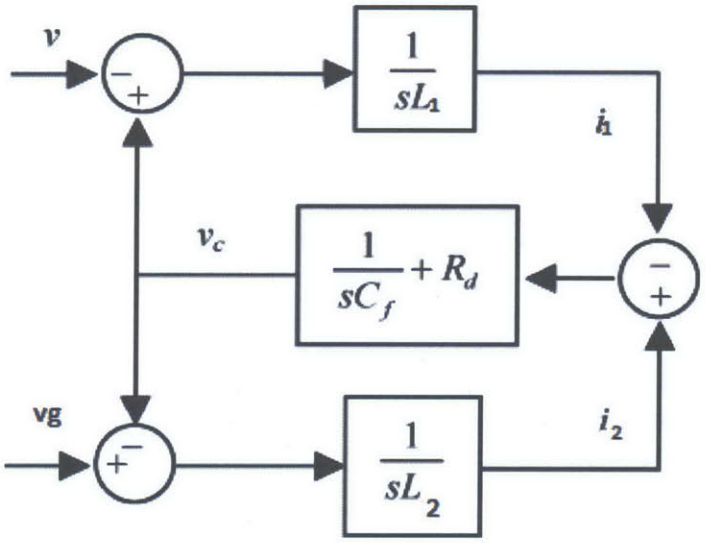

(b) Single-phase mathematical model

Figure 24. Filter Circuit Analysis.

The output filter current is denoted as I_y, and the input filter current is denoted as I_x; the ratio of these two current is used to determine the quality of noise filtering. Its transfer function is derived here

$$\frac{I_y}{I_x} = \frac{\frac{1}{sC_f}||R_d}{sL_f+\left(\frac{1}{sC_f}||R_d\right)} = \frac{R_d}{s^2L_fC_fR_d+sL_f+R_d} = \begin{cases} 1, w \ll w_o \\ -\frac{R_d}{\sqrt{\frac{L_f}{C_f}}}, w = w_o \\ -\frac{1}{w^2L_fC_f}, w \gg w_o \end{cases}.$$

Cut-off frequency is

$$w_o = \frac{L_1 + L_2}{L_1L_2C_f}$$

The bode plot of the transfer function of the L-C filter is shown below, the attenuation is 40dB/dec, and with the L-C-L filter technique, the attenuation can be enhanced up to 60dB/dec.

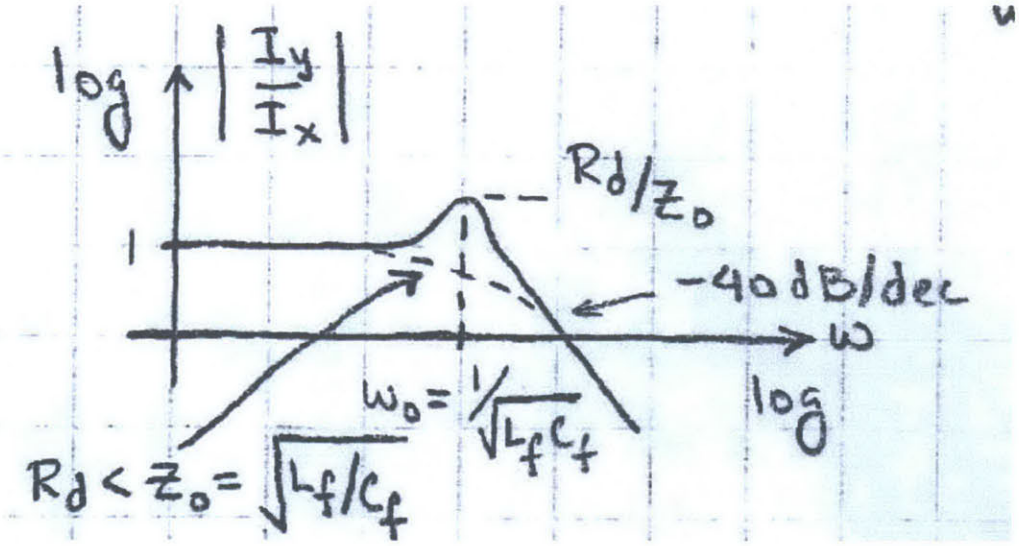

Figure 25. Bode plot of the L-C filter transfer function.

(a) After a series of calculations, values of the filter components are selected below.

(b) 1) 6 x Inductor core: PM 62/48 (please confirm that this is what you used) L1= 1mH, L2 = 0.72mH

(c) 2) 3 x Filter capacitor: 0.33uF, 600V (or higher)

(d) 3) 3 x Damping capacitor: 2uF, 600V (or higher)

(e) 4) 3 x Damping resistor: 60ohms, 10W (or higher)

(f) 5) All other board components (AD8132, etc)

Table 4 Filter Components

Inductors (6)	1mH (3x front)	0.75mH (3x end)
Filter capacitor (3)	1uF AVX 100K 325AD	
Damping Capacitor (3)	3.2uF PHE740MR7220MR05+ AVX 100K 325AD	
Damping resistor (3)	56Ohms OMC TWM5J56R	

A Matlab simulation is performed based on these calculated values, the bode plot of the iy/ix transfer function is shown below, which provides a desired filter quality.

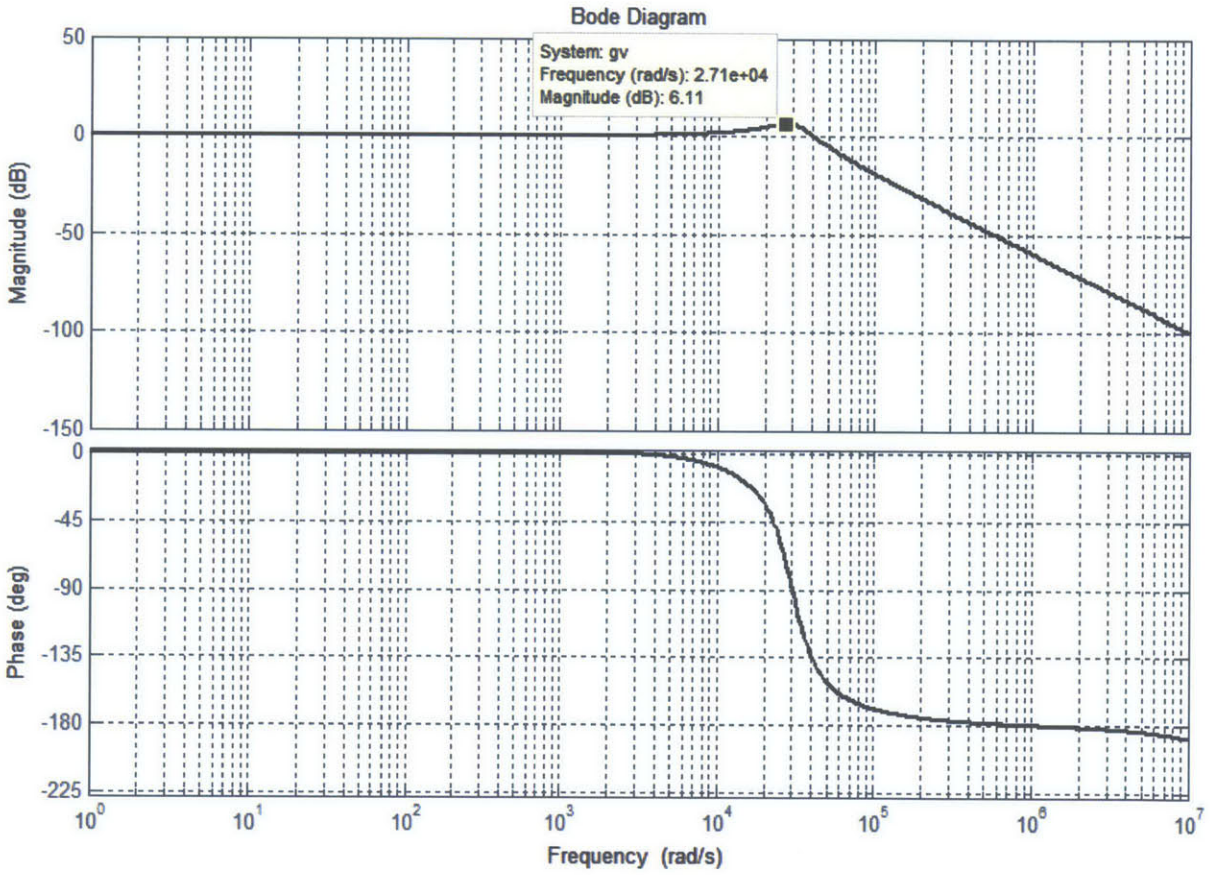

Figure 26. Matlab Simulaiton on the bode plot of the iy/ix transfer function.

Then the next step is to select the components for filter capacitors and inductors. Consider a real capacitor, it has parasitic series resistance and inductance, thus it behave likes a capacitor up to certain frequencies, then looks like a resistor and finally an inductor as high enough frequencies as indicated in the figures below.

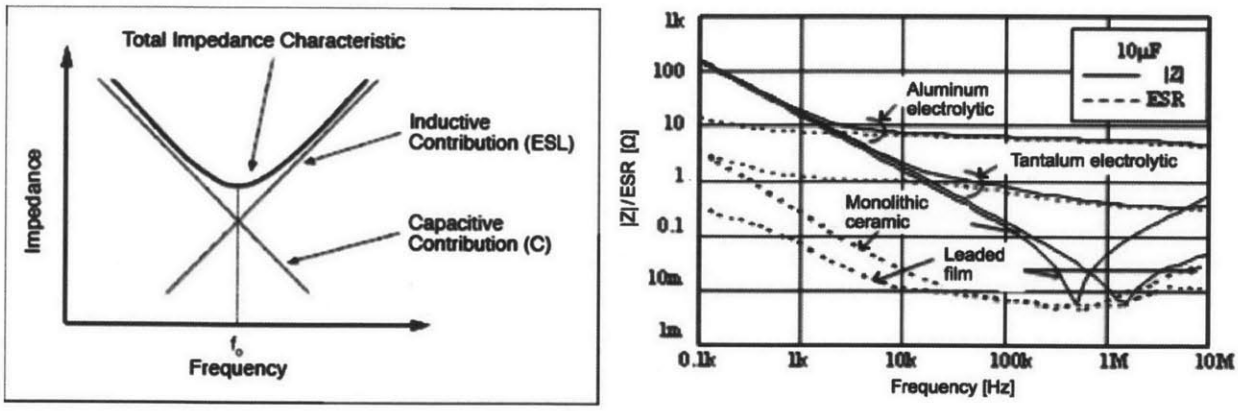

Figure 27. Real Capacitor Impedance vs. Frequency.

The film capacitors are selected due to the high voltage/current power rating, 0.33uF for filter capacitors, and 2uF for damping capacitors.

Next step is the design of filter inductors, and the general procedure is:

a. Given a core geometry and gap, get inductance proportional to turns.

   The selected core is EPOCS PM62/49 which has a gap of 2.6mm. A_L is 315nH. The inductance is proportional to the turns squared.

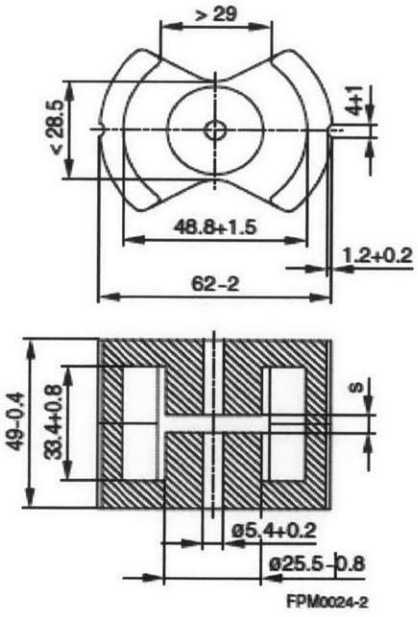

Figure 28. Inductor core PM62/49 B65684A0315A027.

Therefore, for the 1mH inductors, we need (1m/315n)^0.5 = 57 turns; for the 0.75mH inductors, we need (0.75m/315n)^0.5 = 49 turns.

b. We must not exceed the allowed flux density of the material

The flux density of the material is 0.3T.

$$B \geq \frac{L \times i_{L,p}}{NA_C}$$

c. Wire must be thick enough to carry current w/o overheating

$$\frac{i_{LP}}{A_w} \leq \frac{4000A}{cm^2}, A_w = \left(\frac{d}{2}\right)^2 \pi$$

The peak value of inductor current is 50A, so the wire diameter d shall be larger than 1.262mm. Using the reference table below, the author picked AWG 16 (1.29mm) as the inductor coil.

Conversion table - American Wire Gauge - mm. - mm²

AWG N°	Diam. mm.	Area mm²	AWG N°	Diam. mm.	Area mm²
1	7,350	42,400	16	1,290	1,3100
2	6,540	33,600	17	1,150	1,0400
3	5,830	26,700	18	1,024	0,8230
4	5,190	21,200	19	0,912	0,6530
5	4,620	16,800	20	0,812	0,5190
6	4,110	13,300	21	0,723	0,4120
7	3,670	10,600	22	0,644	0,3250
8	3,260	8,350	23	0,573	0,2590
9	2,910	6,620	24	0,511	0,2050
10	2,590	5,270	25	0,455	0,1630
11	2,300	4,150	26	0,405	0,1280
12	2,050	3,310	27	0,361	0,1020
13	1,830	2,630	28	0,321	0,0804
14	1,630	2,080	29	0,286	0,0646
15	1,450	1,650	30	0,255	0,0503

Tnt-Audio Internet HiFi Review http://www.tnt-audio.com

Figure 29. Wire AWG Parameters.

d. Wire must fit in the core window area

As the inductor core is shown in figure 31, the effective area is 570mm².

e. Losses and temperature must be acceptable

$$\text{Winding loss } P_W = {I_{rms}}^2 R_w$$

$$\text{Core power loss } P_{core} = C_M \cdot f^{\alpha} \cdot (B_{ac,pk})^{\beta} \cdot V_{core}$$

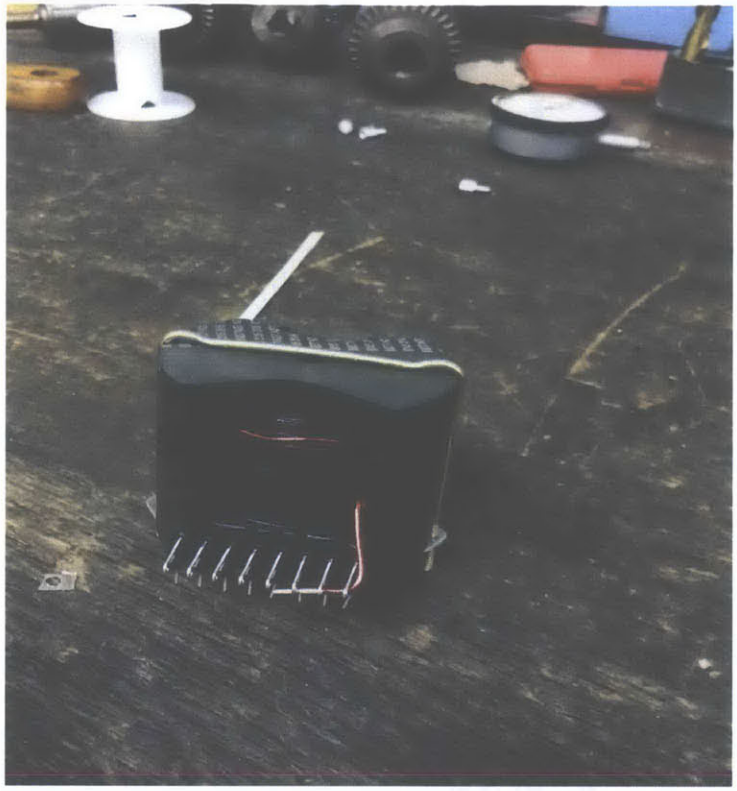

Figure 30. 1mH inductor and its inductance test.

The PCB board is designed in Alitum software, which provides distinguished features of schematic drawing and PCB layout. Its 2D and 3D views are shown in Appendix section B.

The hardware construction has been carried out in the past six months and the following pictures show the professional assembly work. For the safety and integrity concerns, an aluminum packaging box has been purchased to contain the inverter circuit and grid filter circuit.

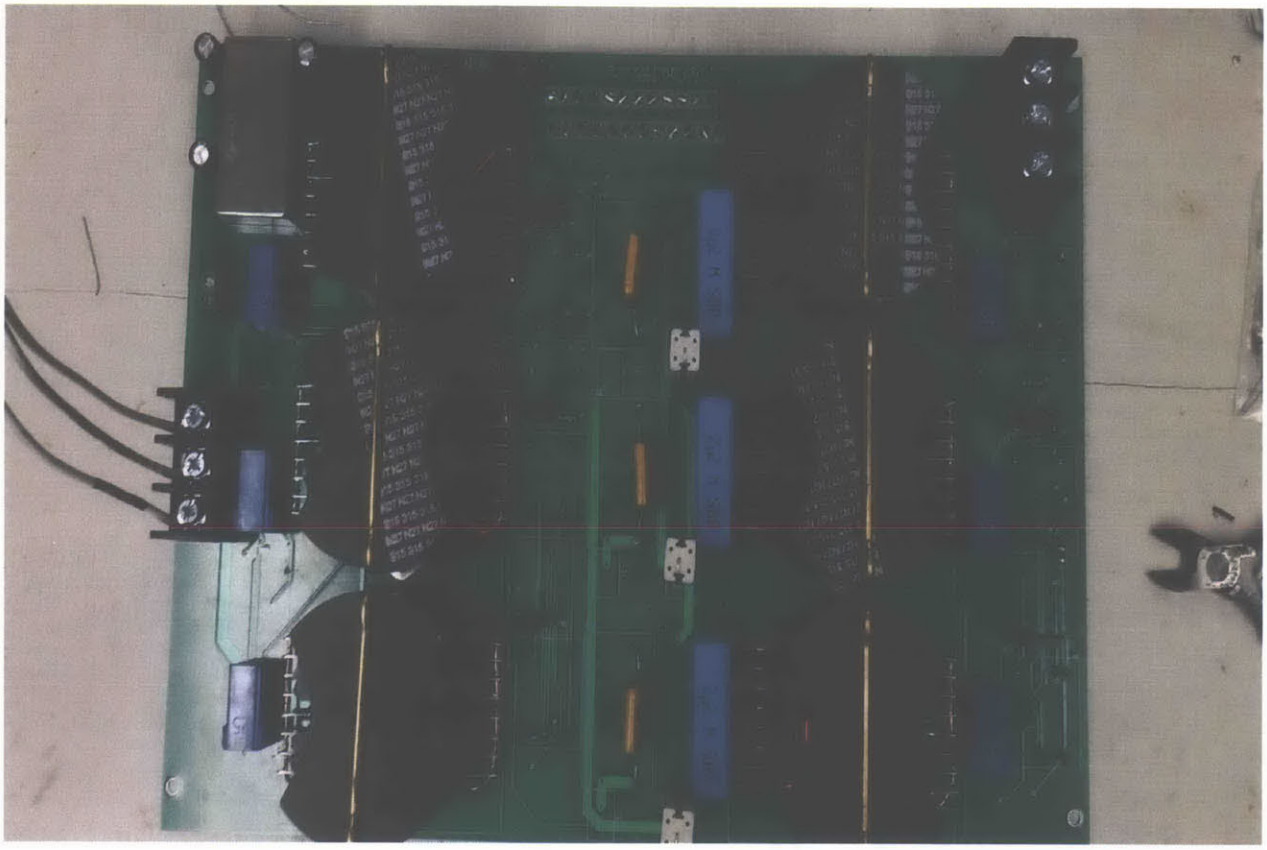

Figure 31. Constructed L-C-L Grid Filter.

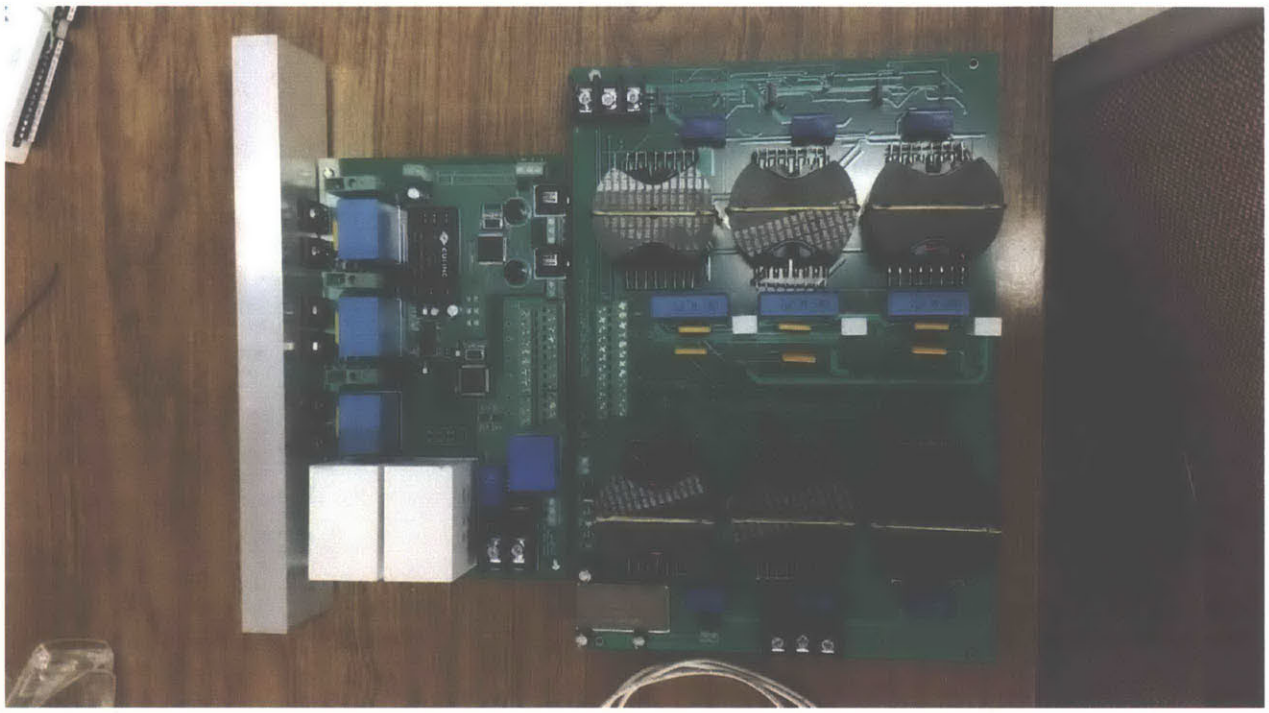

(a). Integrated System without Packaging Box.

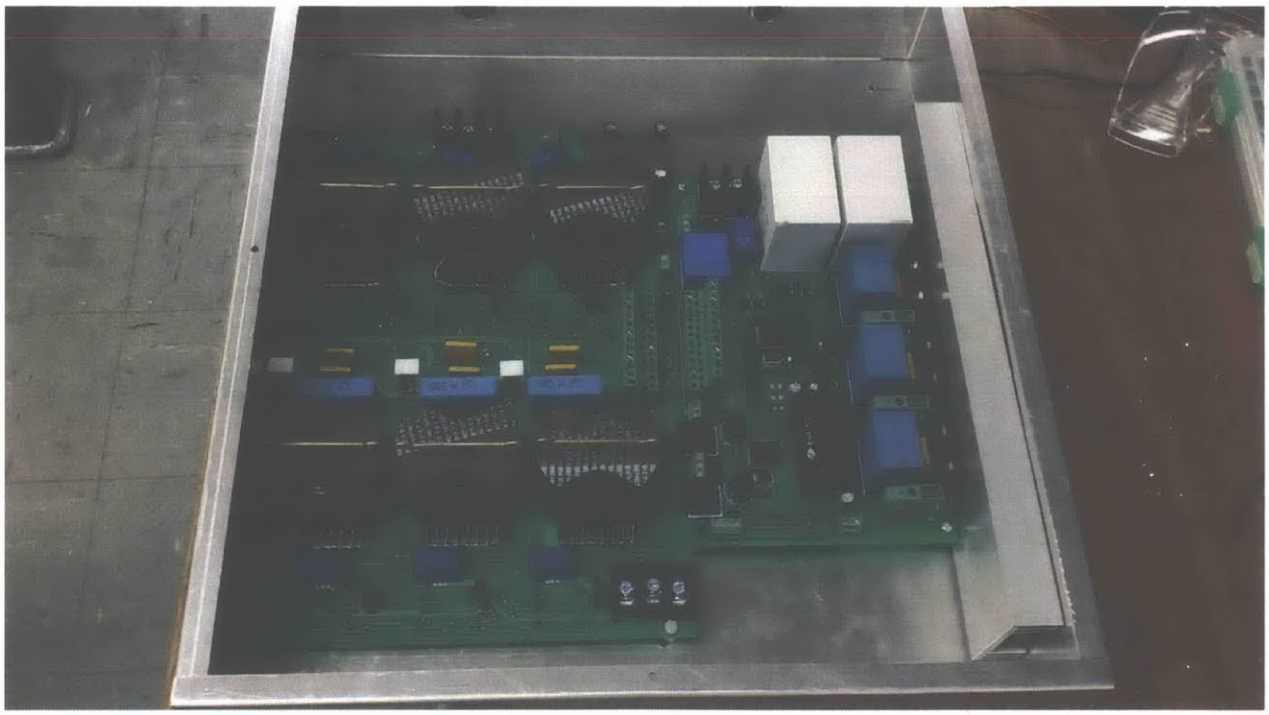

(b). Integrated system with packaging box.

Figure 32. Integrated System (inverter + grid filter).

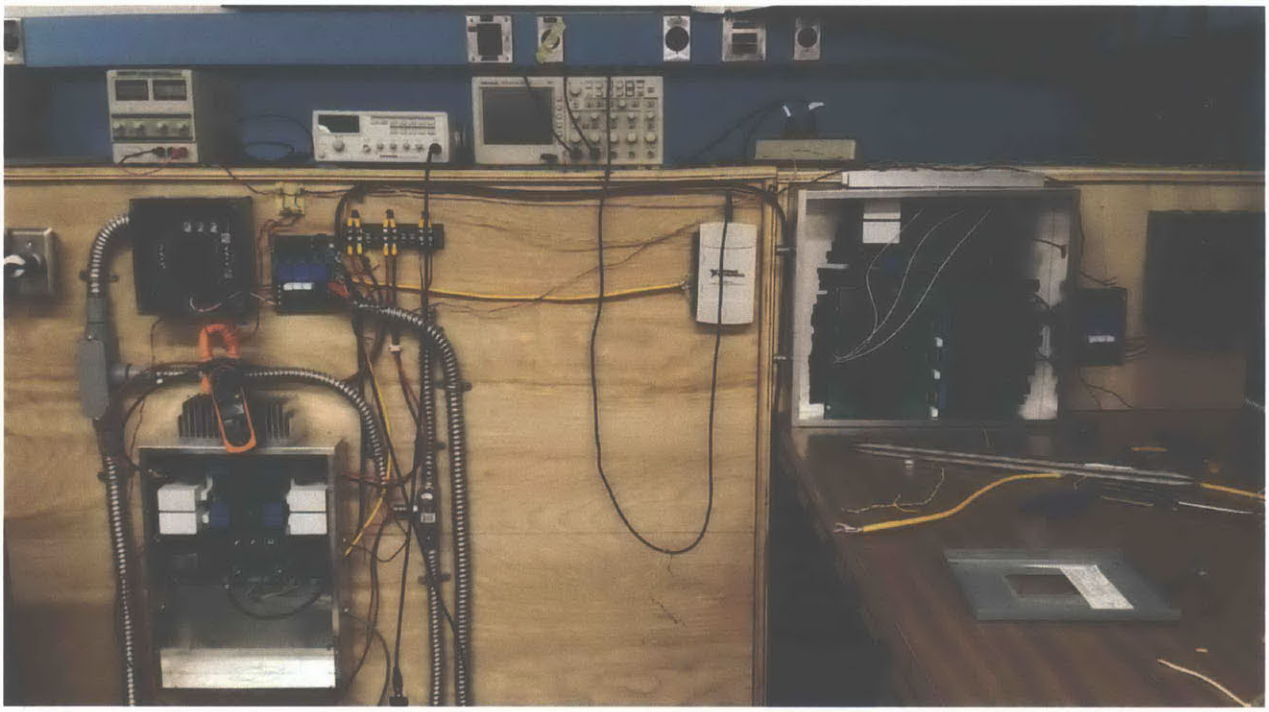

(a) Overall Layout.

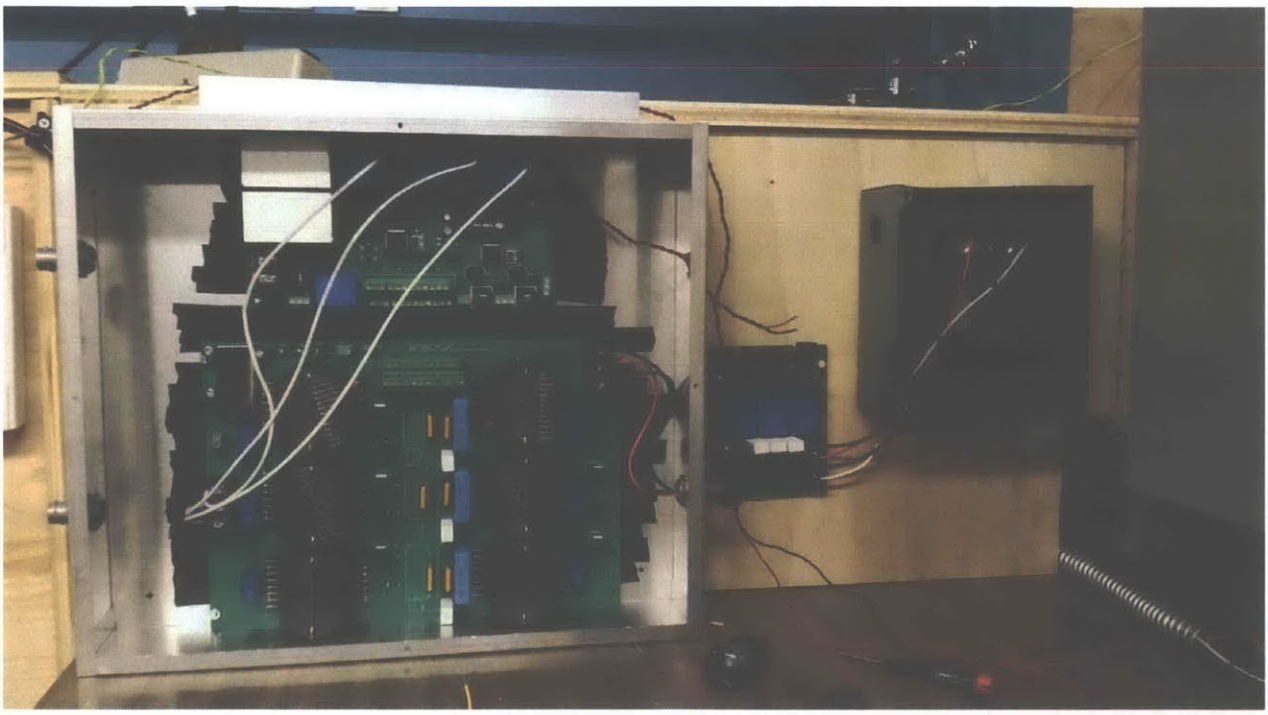

(b) System connected with the grid.

Figure 33. Integrated system set-up with the grid.

Chapter 5 MACHINE TEST

An initial test has been carried out on the generator drive system: 3-phase DC/AC inverter on the grid side with L-C-L filter. The six SVPWM signals were successfully programmed to MOSFET switches and the filter performed well on the noise attenuation.

Through the communication channel of the micro-grid, SVPWM signals are generated to six MOSET switches of the inverter, the duty cycle of one switch is measured in the oscilloscope below.

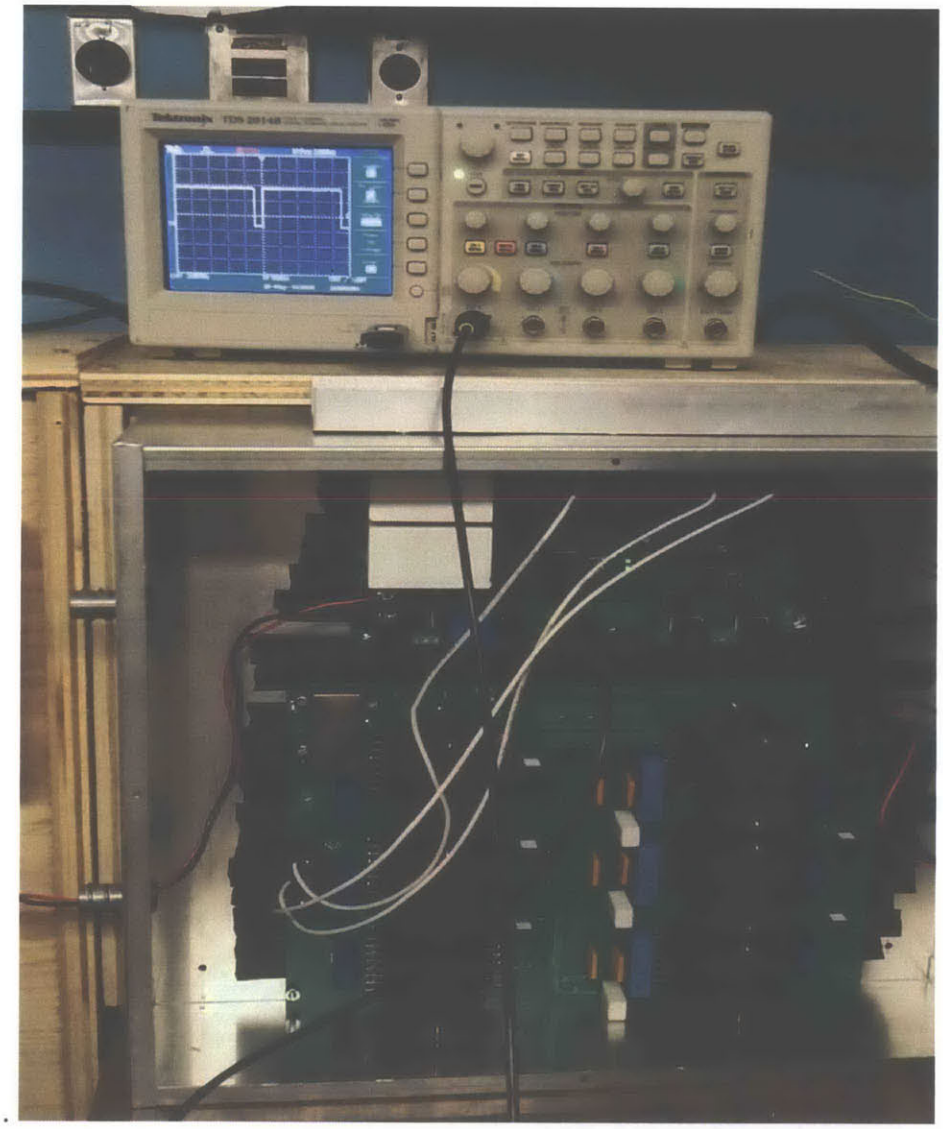

Figure 34. SVPWM generation on the inverter.

A low voltage test has been performed under the condition that the integrated inverter system is connected from the DC power supply to the grid, well filtered three-phase voltages of 15V are acquired using the monitoring board which is placed between the grid filter and the grid.

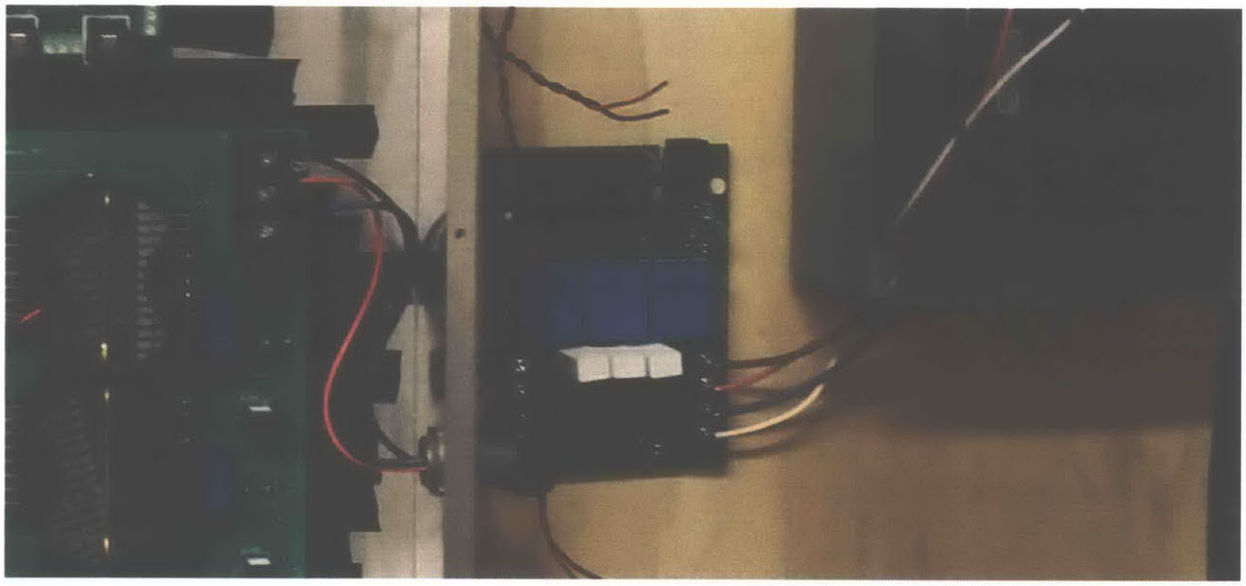

Figure 35. Monitoring Board measuring the voltages.

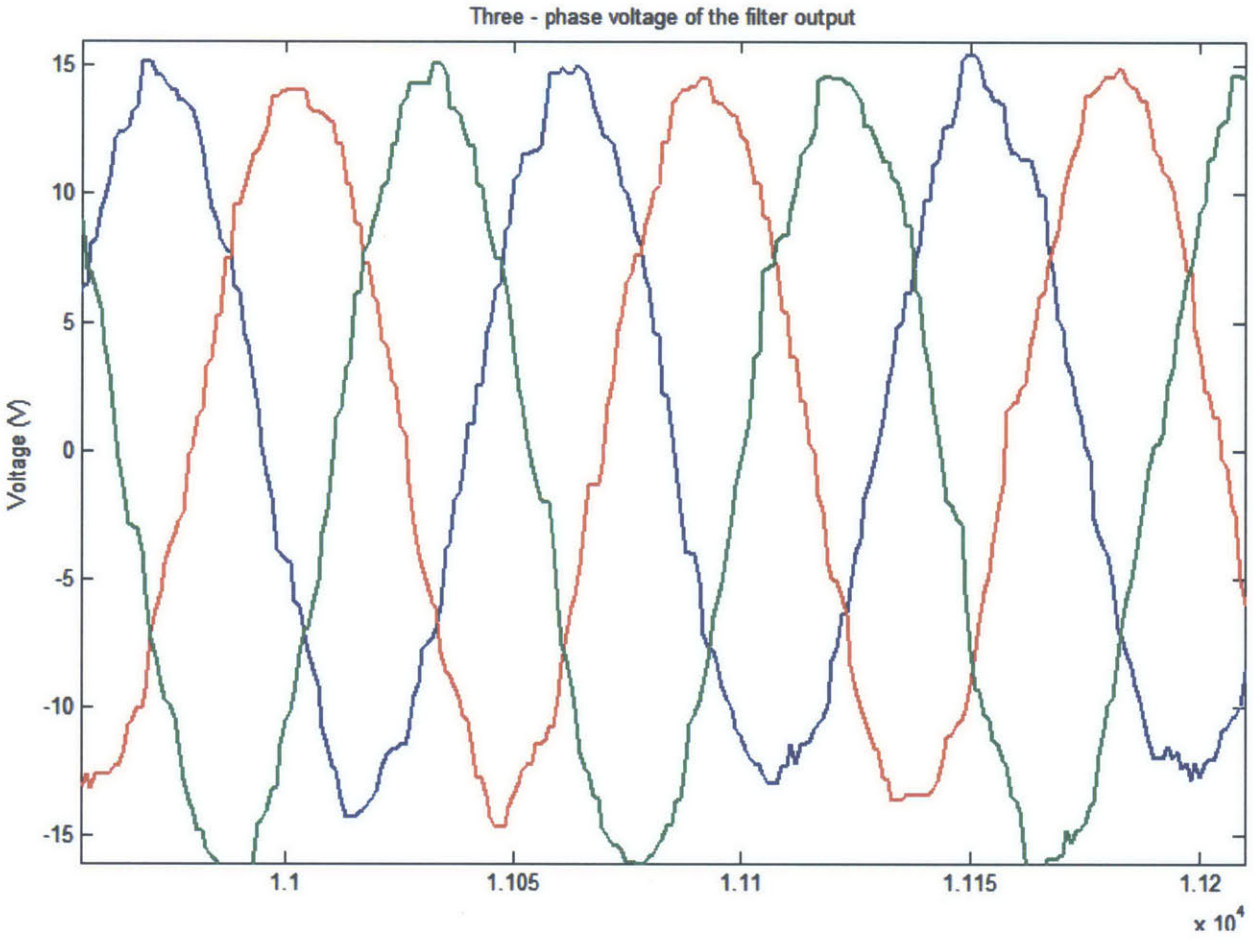

Figure 36. Voltage waveform of the filter output.

Based on the procedures in IEEE Standard 112 and IEEE Standard 113, the parameters of the motors are listed in table 5, which are calculated by previous master students on this project. For the future machine test, a buck converter is designed to drive the 1.5 horsepower DC motor, and the back-to-back inverter is designed to drive the 1 horsepower wound rotor induction motor.

Table 5 Wound Rotor Induction Motor and DC Motor Parameters

Induction Motor	
Stator Leakage X_1	4Ω
Rotor Leakage X_2	4Ω
Magnetizing Reactance X_m	69.3Ω
R_c	469.7Ω

DC Motor	
Armature Resistance	0.7Ω
Armature Inductance	0.032H
Field Resistance	275Ω
Field Inductance	7.5H
Armature to Field Mutual Inductance	2.97H

Chapter 6 CONCLUSION

The purpose of this thesis is to perform an investigation on DIFM to emulate the wind turbine electrical system in the smart micro-grid environment. System modeling and control algorithms have been analyzed and discussed. The comparison study shows that Stator-flux FOC and DTC-SVM are the optimum control algorithms for DFIM.

Extensive efforts have been put into the hardware implementation including the design and construction of the power electronics system.

The initial experiments have been performed to verify both hardware and software set-up are fully functional. This experiment shows a clean three-phase signals are flowing into the grid, which gives a tremendous confidence in the following machine test.

Future work would involve the machine test in different working conditions, including various rotation speed and fault modes (unbalanced grid voltages).

APPENDIX

A. DC/AC Inverter SVPWM generation codes

// The purpose of this C codes is to generate SVPWM signals from the micro-controller to control the six switches on the DC/AC inverter. MPLAB is used as the programming platform.

```
#include <p30F6010A.h>

#include <libpic30.h>

#include <libq.h>

#include <math.h>


/*

        Date: March 10, 2014

        Development Board (dsPICDEM MC1) with pic30F6010A Microcontroller


        Microcontroller: Implementing Space Vector Modulation for inverter

        Note: pic30F has no high and low interrupts. The priority ranges from 0 to 7,

                and each interrupt has to be defined individually.


        This board ties with the microgrid and generates the SVM to generate 3 phase sinusoids with amplitude given
by a


*/


#define _INT __attribute__((__interrupt__, __auto_psv__))


// Configuration settings

_FOSC(CSW_FSCM_OFF & FRC_PLL4);          // Fosc= 16x7.5MHz, Fcy = __MHz

_FWDT(WDT_OFF);                          // Watchdog timer off

_FBORPOR(MCLR_DIS);                      // Disable reset pin


// The following look-up table has 10 elements per degree

// Type "const" saves the table in program memory. Otherwise RAM would be full
```

```
const                    cos_minus_ksin_1024_table[3600]                    =
{1024,1023,1022,1021,1020,1019,1018,1017,1016,1015,1014,1012,1011,1010,1009,1008,1007,1006,1005,1004,10
03,1002,1001,999,998,997,996,995,994,993,992,991,989,988,987,986,985,984,983,981,980,979,978,977,976,974,9
73,972,971,970,969,967,966,965,964,963,961,960,959,958,957,955,954,953,952,950,949,948,947,946,944,943,942,
941,939,938,937,936,934,933,932,930,929,928,927,925,924,923,921,920,919,918,916,915,914,912,911,910,908,90
7,906,904,903,902,900,899,898,896,895,894,892,891,890,\

888,887,886,884,883,881,880,879,877,876,875,873,872,870,869,868,866,865,863,862,861,859,858,856,855,853,85
2,851,849,848,846,845,843,842,840,839,838,836,835,833,832,830,829,827,826,824,823,821,820,818,817,815,814,8
12,811,809,808,806,805,803,802,800,799,797,796,794,793,791,790,788,787,785,783,782,780,779,777,776,774,773,
771,769,768,766,765,763,762,760,758,757,755,754,752,750,749,747,746,744,742,741,739,738,736,734,733,731,73
0,728,726,725,723,721,720,718,717,715,713,712,710,708,\

707,705,703,702,700,698,697,695,693,692,690,688,687,685,683,682,680,678,676,675,673,671,670,668,666,665,66
3,661,659,658,656,654,653,651,649,647,646,644,642,640,639,637,635,634,632,630,628,627,625,623,621,620,618,6
16,614,612,611,609,607,605,604,602,600,598,597,595,593,591,589,588,586,584,582,580,579,577,575,573,571,570,
568,566,564,562,561,559,557,555,553,551,550,548,546,544,542,540,539,537,535,533,531,529,528,526,524,522,52
0,518,516,515,513,511,509,507,505,503,502,500,498,496,\

494,492,490,488,487,485,483,481,479,477,475,473,471,470,468,466,464,462,460,458,456,454,452,451,449,447,44
5,443,441,439,437,435,433,431,429,428,426,424,422,420,418,416,414,412,410,408,406,404,402,400,399,397,395,3
93,391,389,387,385,383,381,379,377,375,373,371,369,367,365,363,361,359,357,356,354,352,350,348,346,344,342,
340,338,336,334,332,330,328,326,324,322,320,318,316,314,312,310,308,306,304,302,300,298,296,294,292,290,28
8,286,284,282,280,278,276,274,272,270,268,266,264,262,\

260,258,256,254,252,250,248,246,244,242,240,238,236,234,232,230,228,226,224,222,219,217,215,213,211,209,20
7,205,203,201,199,197,195,193,191,189,187,185,183,181,179,177,175,173,171,169,167,165,162,160,158,156,154,1
52,150,148,146,144,142,140,138,136,134,132,130,128,126,124,122,119,117,115,113,111,109,107,105,103,101,99,9
7,95,93,91,89,87,84,82,80,78,76,74,72,70,68,66,64,62,60,58,56,54,52,49,47,45,43,41,39,37,35,33,31,29,27,25,23,21
,19,16,14,12,10,8,6,4,2,0,-2,-4,-6,-8,-10,-12,-14,-17,-19,\

-21,-23,-25,-27,-29,-31,-33,-35,-37,-39,-41,-43,-45,-47,-50,-52,-54,-56,-58,-60,-62,-64,-66,-68,-70,-72,-74,-76,-78,-
80,-83,-85,-87,-89,-91,-93,-95,-97,-99,-101,-103,-105,-107,-109,-111,-113,-115,-117,-120,-122,-124,-126,-128,-
130,-132,-134,-136,-138,-140,-142,-144,-146,-148,-150,-152,-154,-156,-158,-161,-163,-165,-167,-169,-171,-173,-
175,-177,-179,-181,-183,-185,-187,-189,-191,-193,-195,-197,-199,-201,-203,-205,-207,-209,-211,-213,-216,-218,-
220,-222,-224,-226,-228,-230,-232,-234,-236,-238,-240,-242,\

-244,-246,-248,-250,-252,-254,-256,-258,-260,-262,-264,-266,-268,-270,-272,-274,-276,-278,-280,-282,-284,-286,-
288,-290,-292,-294,-296,-298,-300,-302,-304,-306,-308,-310,-312,-314,-316,-318,-320,-322,-324,-326,-328,-330,-
332,-334,-336,-338,-340,-342,-344,-346,-348,-350,-352,-354,-356,-358,-360,-362,-363,-365,-367,-369,-371,-373,-
375,-377,-379,-381,-383,-385,-387,-389,-391,-393,-395,-397,-399,-401,-403,-404,-406,-408,-410,-412,-414,-416,-
418,-420,-422,-424,-426,-428,-430,-431,-433,-435,-437,-439,\

-441,-443,-445,-447,-449,-451,-453,-454,-456,-458,-460,-462,-464,-466,-468,-470,-472,-473,-475,-477,-479,-481,-
483,-485,-487,-489,-490,-492,-494,-496,-498,-500,-502,-503,-505,-507,-509,-511,-513,-515,-517,-518,-520,-522,-
524,-526,-528,-529,-531,-533,-535,-537,-539,-541,-542,-544,-546,-548,-550,-552,-553,-555,-557,-559,-561,-562,-
564,-566,-568,-570,-571,-573,-575,-577,-579,-581,-582,-584,-586,-588,-589,-591,-593,-595,-597,-598,-600,-602,-
604,-605,-607,-609,-611,-613,-614,-616,-618,-620,-621,-623,\

-625,-627,-628,-630,-632,-634,-635,-637,-639,-641,-642,-644,-646,-647,-649,-651,-653,-654,-656,-658,-660,-661,-
663,-665,-666,-668,-670,-671,-673,-675,-677,-678,-680,-682,-683,-685,-687,-688,-690,-692,-693,-695,-697,-698,-
700,-702,-703,-705,-707,-708,-710,-712,-713,-715,-717,-718,-720,-721,-723,-725,-726,-728,-730,-731,-733,-735,-
```

736,-738,-739,-741,-743,-744,-746,-747,-749,-751,-752,-754,-755,-757,-759,-760,-762,-763,-765,-766,-768,-770,-771,-773,-774,-776,-777,-779,-780,-782,-784,-785,-787,-788,\

-790,-791,-793,-794,-796,-797,-799,-800,-802,-803,-805,-806,-808,-809,-811,-812,-814,-815,-817,-818,-820,-821,-823,-824,-826,-827,-829,-830,-832,-833,-835,-836,-838,-839,-841,-842,-843,-845,-846,-848,-849,-851,-852,-853,-855,-856,-858,-859,-861,-862,-863,-865,-866,-868,-869,-870,-872,-873,-875,-876,-877,-879,-880,-882,-883,-884,-886,-887,-888,-890,-891,-892,-894,-895,-896,-898,-899,-901,-902,-903,-905,-906,-907,-908,-910,-911,-912,-914,-915,-916,-918,-919,-920,-922,-923,-924,-925,-927,-928,-929,\

-931,-932,-933,-934,-936,-937,-938,-939,-941,-942,-943,-944,-946,-947,-948,-949,-951,-952,-953,-954,-955,-957,-958,-959,-960,-961,-963,-964,-965,-966,-967,-969,-970,-971,-972,-973,-975,-976,-977,-978,-979,-980,-981,-983,-984,-985,-986,-987,-988,-989,-991,-992,-993,-994,-995,-996,-997,-998,-999,-1001,-1002,-1003,-1004,-1005,-1006,-1007,-1008,-1009,-1010,-1011,-1013,-1014,-1015,-1016,-1017,-1018,-1019,-1020,-1021,-1022,-1023,-1024,-1025,-1026,-1027,-1028,-1029,-1030,-1031,-1032,-1033,-1034,\

-1035,-1036,-1037,-1038,-1039,-1040,-1041,-1042,-1043,-1044,-1045,-1046,-1047,-1048,-1049,-1050,-1051,-1052,-1053,-1054,-1055,-1055,-1056,-1057,-1058,-1059,-1060,-1061,-1062,-1063,-1064,-1065,-1065,-1066,-1067,-1068,-1069,-1070,-1071,-1072,-1073,-1073,-1074,-1075,-1076,-1077,-1078,-1079,-1079,-1080,-1081,-1082,-1083,-1084,-1084,-1085,-1086,-1087,-1088,-1088,-1089,-1090,-1091,-1092,-1092,-1093,-1094,-1095,-1096,-1096,-1097,-1098,-1099,-1099,-1100,-1101,-1102,-1102,-1103,-1104,\

-1105,-1105,-1106,-1107,-1108,-1108,-1109,-1110,-1110,-1111,-1112,-1113,-1113,-1114,-1115,-1115,-1116,-1117,-1117,-1118,-1119,-1119,-1120,-1121,-1121,-1122,-1123,-1123,-1124,-1125,-1125,-1126,-1126,-1127,-1128,-1128,-1129,-1130,-1130,-1131,-1131,-1132,-1133,-1133,-1134,-1134,-1135,-1136,-1136,-1137,-1137,-1138,-1138,-1139,-1139,-1140,-1141,-1141,-1142,-1142,-1143,-1143,-1144,-1144,-1145,-1145,-1146,-1146,-1147,-1147,-1148,-1148,-1149,-1149,-1150,-1150,-1151,-1151,-1152,-1152,\

-1153,-1153,-1154,-1154,-1154,-1155,-1155,-1156,-1156,-1157,-1157,-1157,-1158,-1158,-1159,-1159,-1160,-1160,-1160,-1161,-1161,-1162,-1162,-1162,-1163,-1163,-1163,-1164,-1164,-1164,-1165,-1165,-1166,-1166,-1166,-1167,-1167,-1167,-1168,-1168,-1168,-1169,-1169,-1169,-1169,-1170,-1170,-1170,-1171,-1171,-1171,-1172,-1172,-1172,-1172,-1173,-1173,-1173,-1173,-1174,-1174,-1174,-1174,-1175,-1175,-1175,-1175,-1176,-1176,-1176,-1176,-1176,-1177,-1177,-1177,-1177,-1177,-1178,-1178,-1178,\

-1178,-1178,-1178,-1179,-1179,-1179,-1179,-1179,-1179,-1180,-1180,-1180,-1180,-1180,-1180,-1180,-1180,-1181,-1181,-1181,-1181,-1181,-1181,-1181,-1181,-1181,-1181,-1182,-1181,-1181,-1181,-1181,-1181,-1181,-1181,-1181,\

-1181,-1181,-1180,-1180,-1180,-1180,-1180,-1180,-1180,-1180,-1179,-1179,-1179,-1179,-1179,-1179,-1178,-1178,-1178,-1178,-1178,-1178,-1177,-1177,-1177,-1177,-1177,-1176,-1176,-1176,-1176,-1176,-1175,-1175,-1175,-1175,-1174,-1174,-1174,-1174,-1173,-1173,-1173,-1173,-1172,-1172,-1172,-1171,-1171,-1171,-1171,-1170,-1170,-1170,-1169,-1169,-1169,-1169,-1168,-1168,-1168,-1167,-1167,-1167,-1166,-1166,-1166,-1165,-1165,-1164,-1164,-1164,-1163,-1163,-1163,-1162,-1162,-1161,-1161,-1161,\

-1160,-1160,-1160,-1159,-1159,-1158,-1158,-1157,-1157,-1157,-1156,-1156,-1155,-1155,-1154,-1154,-1154,-1153,-1153,-1152,-1152,-1151,-1151,-1150,-1150,-1149,-1149,-1148,-1148,-1147,-1147,-1146,-1146,-1145,-1145,-1144,-1144,-1143,-1143,-1142,-1142,-1141,-1141,-1140,-1139,-1139,-1138,-1138,-1137,-1137,-1136,-1135,-1135,-1134,-1134,-1133,-1133,-1132,-1131,-1131,-1130,-1130,-1129,-1128,-1128,-1127,-1126,-1126,-1125,-1125,-1124,-1123,-1123,-1122,-1121,-1121,-1120,-1119,-1119,-1118,\

-1117,-1117,-1116,-1115,-1115,-1114,-1113,-1113,-1112,-1111,-1110,-1110,-1109,-1108,-1108,-1107,-1106,-1105,-1105,-1104,-1103,-1102,-1102,-1101,-1100,-1099,-1099,-1098,-1097,-1096,-1096,-1095,-1094,-1093,-1092,-1092,-1091,-1090,-1089,-1088,-1088,-1087,-1086,-1085,-1084,-1084,-1083,-1082,-1081,-1080,-1079,-1079,-1078,-

1077,-1076,-1075,-1074,-1073,-1073,-1072,-1071,-1070,-1069,-1068,-1067,-1066,-1065,-1065,-1064,-1063,-1062,-1061,-1060,-1059,-1058,-1057,-1056,-1055,-1054,-1054,\

-1053,-1052,-1051,-1050,-1049,-1048,-1047,-1046,-1045,-1044,-1043,-1042,-1041,-1040,-1039,-1038,-1037,-1036,-1035,-1034,-1033,-1032,-1031,-1030,-1029,-1028,-1027,-1026,-1025,-1024,-1023,-1022,-1021,-1020,-1019,-1018,-1017,-1016,-1015,-1014,-1012,-1011,-1010,-1009,-1008,-1007,-1006,-1005,-1004,-1003,-1002,-1001,-999,-998,-997,-996,-995,-994,-993,-992,-991,-989,-988,-987,-986,-985,-984,-983,-981,-980,-979,-978,-977,-976,-974,-973,-972,-971,-970,-969,-967,-966,-965,-964,-963,-961,-960,\

-959,-958,-957,-955,-954,-953,-952,-950,-949,-948,-947,-946,-944,-943,-942,-941,-939,-938,-937,-936,-934,-933,-932,-930,-929,-928,-927,-925,-924,-923,-921,-920,-919,-918,-916,-915,-914,-912,-911,-910,-908,-907,-906,-904,-903,-902,-900,-899,-898,-896,-895,-894,-892,-891,-890,-888,-887,-886,-884,-883,-881,-880,-879,-877,-876,-875,-873,-872,-870,-869,-868,-866,-865,-863,-862,-861,-859,-858,-856,-855,-853,-852,-851,-849,-848,-846,-845,-843,-842,-840,-839,-838,-836,-835,-833,-832,-830,-829,-827,-826,\

-824,-823,-821,-820,-818,-817,-815,-814,-812,-811,-809,-808,-806,-805,-803,-802,-800,-799,-797,-796,-794,-793,-791,-790,-788,-787,-785,-783,-782,-780,-779,-777,-776,-774,-773,-771,-769,-768,-766,-765,-763,-762,-760,-758,-757,-755,-754,-752,-750,-749,-747,-746,-744,-742,-741,-739,-738,-736,-734,-733,-731,-730,-728,-726,-725,-723,-721,-720,-718,-717,-715,-713,-712,-710,-708,-707,-705,-703,-702,-700,-698,-697,-695,-693,-692,-690,-688,-687,-685,-683,-682,-680,-678,-676,-675,-673,-671,-670,-668,-666,\

-665,-663,-661,-659,-658,-656,-654,-653,-651,-649,-647,-646,-644,-642,-640,-639,-637,-635,-634,-632,-630,-628,-627,-625,-623,-621,-620,-618,-616,-614,-612,-611,-609,-607,-605,-604,-602,-600,-598,-597,-595,-593,-591,-589,-588,-586,-584,-582,-580,-579,-577,-575,-573,-571,-570,-568,-566,-564,-562,-561,-559,-557,-555,-553,-551,-550,-548,-546,-544,-542,-540,-539,-537,-535,-533,-531,-529,-528,-526,-524,-522,-520,-518,-516,-515,-513,-511,-509,-507,-505,-503,-502,-500,-498,-496,-494,-492,-490,-488,-487,\

-485,-483,-481,-479,-477,-475,-473,-471,-470,-468,-466,-464,-462,-460,-458,-456,-454,-452,-451,-449,-447,-445,-443,-441,-439,-437,-435,-433,-431,-429,-428,-426,-424,-422,-420,-418,-416,-414,-412,-410,-408,-406,-404,-402,-400,-399,-397,-395,-393,-391,-389,-387,-385,-383,-381,-379,-377,-375,-373,-371,-369,-367,-365,-363,-361,-359,-357,-356,-354,-352,-350,-348,-346,-344,-342,-340,-338,-336,-334,-332,-330,-328,-326,-324,-322,-320,-318,-316,-314,-312,-310,-308,-306,-304,-302,-300,-298,-296,-294,-292,\

-290,-288,-286,-284,-282,-280,-278,-276,-274,-272,-270,-268,-266,-264,-262,-260,-258,-256,-254,-252,-250,-248,-246,-244,-242,-240,-238,-236,-234,-232,-230,-228,-226,-224,-222,-219,-217,-215,-213,-211,-209,-207,-205,-203,-201,-199,-197,-195,-193,-191,-189,-187,-185,-183,-181,-179,-177,-175,-173,-171,-169,-167,-165,-162,-160,-158,-156,-154,-152,-150,-148,-146,-144,-142,-140,-138,-136,-134,-132,-130,-128,-126,-124,-122,-119,-117,-115,-113,-111,-109,-107,-105,-103,-101,-99,-97,-95,-93,-91,-89,-87,-84,\

-82,-80,-78,-76,-74,-72,-70,-68,-66,-64,-62,-60,-58,-56,-54,-52,-49,-47,-45,-43,-41,-39,-37,-35,-33,-31,-29,-27,-25,-23,-21,-19,-16,-14,-12,-10,-8,-6,-4,-
2,0,2,4,6,8,10,12,14,17,19,21,23,25,27,29,31,33,35,37,39,41,43,45,47,50,52,54,56,58,60,62,64,66,68,70,72,74,76,78,80,83,85,87,89,91,93,95,97,99,101,103,105,107,109,111,113,115,117,120,122,124,126,128,130,132,134,136,138,140,142,144,146,148,150,152,154,156,158,161,163,165,167,169,171,173,175,177,\

179,181,183,185,187,189,191,193,195,197,199,201,203,205,207,209,211,213,216,218,220,222,224,226,228,230,232,234,236,238,240,242,244,246,248,250,252,254,256,258,260,262,264,266,268,270,272,274,276,278,280,282,284,286,288,290,292,294,296,298,300,302,304,306,308,310,312,314,316,318,320,322,324,326,328,330,332,334,336,338,340,342,344,346,348,350,352,354,356,358,360,362,363,365,367,369,371,373,375,377,379,381,383,385,387,389,391,393,395,397,399,401,403,404,406,408,410,412,414,416,\

418,420,422,424,426,428,430,431,433,435,437,439,441,443,445,447,449,451,453,454,456,458,460,462,464,466,468,470,472,473,475,477,479,481,483,485,487,489,490,492,494,496,498,500,502,503,505,507,509,511,513,515,517,518,520,522,524,526,528,529,531,533,535,537,539,541,542,544,546,548,550,552,553,555,557,559,561,562,564,566,

568,570,571,573,575,577,579,581,582,584,586,588,589,591,593,595,597,598,600,602,604,605,607,609,611,613,61
4,616,618,620,621,623,625,627,628,630,632,634,635,637,\

639,641,642,644,646,647,649,651,653,654,656,658,660,661,663,665,666,668,670,671,673,675,677,678,680,682,68
3,685,687,688,690,692,693,695,697,698,700,702,703,705,707,708,710,712,713,715,717,718,720,721,723,725,726,7
28,730,731,733,735,736,738,739,741,743,744,746,747,749,751,752,754,755,757,759,760,762,763,765,766,768,770,
771,773,774,776,777,779,780,782,784,785,787,788,790,791,793,794,796,797,799,800,802,803,805,806,808,809,81
1,812,814,815,817,818,820,821,823,824,826,827,829,830,\

832,833,835,836,838,839,841,842,843,845,846,848,849,851,852,853,855,856,858,859,861,862,863,865,866,868,86
9,870,872,873,875,876,877,879,880,882,883,884,886,887,888,890,891,892,894,895,896,898,899,901,902,903,905,9
06,907,908,910,911,912,914,915,916,918,919,920,922,923,924,925,927,928,929,931,932,933,934,936,937,938,939,
941,942,943,944,946,947,948,949,951,952,953,954,955,957,958,959,960,961,963,964,965,966,967,969,970,971,97
2,973,975,976,977,978,979,980,981,983,984,985,986,987,\

988,989,991,992,993,994,995,996,997,998,999,1001,1002,1003,1004,1005,1006,1007,1008,1009,1010,1011,1013,1
014,1015,1016,1017,1018,1019,1020,1021,1022,1023,1024,1025,1026,1027,1028,1029,1030,1031,1032,1033,1034,
1035,1036,1037,1038,1039,1040,1041,1042,1043,1044,1045,1046,1047,1048,1049,1050,1051,1052,1053,1054,105
5,1055,1056,1057,1058,1059,1060,1061,1062,1063,1064,1065,1065,1066,1067,1068,1069,1070,1071,1072,1073,10
73,1074,1075,1076,1077,1078,1079,1079,1080,1081,\

1082,1083,1084,1084,1085,1086,1087,1088,1088,1089,1090,1091,1092,1092,1093,1094,1095,1096,1096,1097,109
8,1099,1099,1100,1101,1102,1102,1103,1104,1105,1105,1106,1107,1108,1108,1109,1110,1110,1111,1112,1113,11
13,1114,1115,1115,1116,1117,1117,1118,1119,1119,1120,1121,1121,1122,1123,1123,1124,1125,1125,1126,1126,1
127,1128,1128,1129,1130,1130,1131,1131,1132,1133,1133,1134,1134,1135,1136,1136,1137,1137,1138,1138,1139,
1139,1140,1141,1141,1142,1142,1143,1143,1144,1144,\

1145,1145,1146,1146,1147,1147,1148,1148,1149,1149,1150,1150,1151,1151,1152,1152,1153,1153,1154,1154,115
4,1155,1155,1156,1156,1157,1157,1157,1158,1158,1159,1159,1160,1160,1160,1161,1161,1162,1162,1162,1163,11
63,1163,1164,1164,1164,1165,1165,1166,1166,1166,1167,1167,1167,1168,1168,1168,1169,1169,1169,1169,1170,1
170,1170,1171,1171,1171,1172,1172,1172,1172,1173,1173,1173,1173,1174,1174,1174,1174,1175,1175,1175,1175,
1176,1176,1176,1176,1176,1177,1177,1177,1177,1177,\

1178,1178,1178,1178,1178,1178,1179,1179,1179,1179,1179,1179,1180,1180,1180,1180,1180,1180,1180,1180,118
1,1181,1181,1181,1181,1181,1181,1181,1181,1181,1182,1182,1182,1182,1182,1182,1182,1182,1182,1182,1182,11
82,1182,1182,1182,1182,1182,1182,1182,1182,1182,1182,1182,1182,1182,1182,1182,1182,1182,1182,1182,1182,1
182,1182,1182,1182,1182,1182,1182,1182,1182,1182,1182,1182,1182,1181,1181,1181,1181,1181,1181,1181,1181,
1181,1181,1180,1180,1180,1180,1180,1180,1180,1180,\

1179,1179,1179,1179,1179,1179,1178,1178,1178,1178,1178,1178,1177,1177,1177,1177,1177,1176,1176,1176,117
6,1176,1175,1175,1175,1175,1174,1174,1174,1174,1173,1173,1173,1173,1172,1172,1172,1171,1171,1171,1171,11
70,1170,1170,1169,1169,1169,1169,1168,1168,1168,1167,1167,1167,1166,1166,1166,1165,1165,1164,1164,1164,1
163,1163,1163,1162,1162,1161,1161,1161,1160,1160,1160,1159,1159,1158,1158,1157,1157,1157,1156,1156,1155,
1155,1154,1154,1154,1153,1153,1152,1152,1151,1151,\

1150,1150,1149,1149,1148,1148,1147,1147,1146,1146,1145,1145,1144,1144,1143,1143,1142,1142,1141,1141,114
0,1139,1139,1138,1138,1137,1137,1136,1135,1135,1134,1134,1133,1133,1132,1131,1131,1130,1130,1129,1128,11
28,1127,1126,1126,1125,1125,1124,1123,1123,1122,1121,1121,1120,1119,1119,1118,1117,1117,1116,1115,1115,1
114,1113,1113,1112,1111,1110,1110,1109,1108,1108,1107,1106,1105,1105,1104,1103,1102,1102,1101,1100,1099,
1099,1098,1097,1096,1096,1095,1094,1093,1092,1092,\

1091,1090,1089,1088,1088,1087,1086,1085,1084,1084,1083,1082,1081,1080,1079,1079,1078,1077,1076,1075,107
4,1073,1073,1072,1071,1070,1069,1068,1067,1066,1065,1065,1064,1063,1062,1061,1060,1059,1058,1057,1056,10
55,1054,1054,1053,1052,1051,1050,1049,1048,1047,1046,1045,1044,1043,1042,1041,1040,1039,1038,1037,1036,1
035,1034,1033,1032,1031,1030,1029,1028,1027,1026,1025};

```
int i, j, k;                    // Previously we had 3 seperate look-up tables, which have the
                                // same information 60 degrees out of phase. Now we
just use one look-up table
                                // with three index integers 60 degrees apart. These
access the corresponding information of the table
                                // 60 degrees apart. For example, when i=1200 (ie
i=120 deg) then j=600 (ie j=60 deg) and k=0 (k=0 deg)
char flag1;
signed long d1, d2, d0;
signed long P1, P2, P3;
long m;                         // Modulation index
float w;                        // Frequency
float phi;                      // Angle
_Q16 PWMfact;                   // Factor to implement duty cycle

_Q16 a;
_Q16 b;

void _INT _PWMInterrupt(void)
                                // PWM interrupt determines how often we update the
duty cycle of each output
{
        flag1 = 1;              // We try to keep all calculations out of the Interrupt Service
Routine
                                // Our approach is to create flag variables that activate
certain chunks of
                                // code in the main while loop. This is done using
if(flag1){...action...}
        IFS2bits.PWMIF = 0;
}

void Configuration(void)
{
```

```
                                                    // 1.1) Configure I/O pins
        TRISAbits.TRISA9 = 0;
        TRISAbits.TRISA10 = 0;
        TRISAbits.TRISA14 = 0;
        TRISAbits.TRISA15 = 0;
        TRISDbits.TRISD11 = 0;

        IEC2bits.PWMIE = 1;
        IFS2bits.PWMIF = 0;


// Configure the PWM
// PTCON register
        PTCONbits.PTEN = 1;                         // Turn on the PWM Time Base
Timer
        PTCONbits.PTOPS = 0;                        // Postscaler of 1
        PTCONbits.PTCKPS = 0b00;                    // Prescaler is 1 so that timer is TCY
        PTCONbits.PTMOD = 0b10;                     // Time base operates in a
continuous up/down counting mode

// PTPER register
        PTPERbits.PTPER = 812;                      // Set the period

// PWMCON1 register
        PWMCON1bits.PMOD1 = 0;                      // PWM1 operates in
complementary mode
        PWMCON1bits.PEN1H = 1;                      // Enable PWM1 high output
        PWMCON1bits.PEN1L = 1;                      // Enable PWM1 low output

        PWMCON1bits.PMOD2 = 0;                      // PWM2 operates in
complementary mode
        PWMCON1bits.PEN2H = 1;                      // Enable PWM2 high output
        PWMCON1bits.PEN2L = 1;                      // Enable PWM2 low output
```

```
        PWMCON1bits.PMOD3 = 0;                  // PWM3 operates in
complementary mode
        PWMCON1bits.PEN3H = 1;                  // Enable PWM3 high output
        PWMCON1bits.PEN3L = 1;                  // Enable PWM3 low output

        PWMCON1bits.PMOD4 = 0;                  // PWM4 operates in
complementary mode
        PWMCON1bits.PEN4H = 0;                  // Disable PWM4 high output
        PWMCON1bits.PEN4L = 0;                  // Disable PWM4 low output

// PWMCON2 register
        PWMCON2bits.UDIS = 0;                   // Updates from duty cycle and
period buffer register enabled

// DTCON1 register
        DTCON1bits.DTBPS = 0b10;            // Prescaler for dead time unit B is 1
        DTCON1bits.DTB = 5;                     // No dead time for now
        DTCON1bits.DTAPS = 0b10;            // Prescaler for dead time unit A is 1
        DTCON1bits.DTA = 5;                     // No dead time for now

// DTCON2 register
        DTCON2bits.DTS4A = 1;
        DTCON2bits.DTS4I = 1;
        DTCON2bits.DTS3A = 1;
        DTCON2bits.DTS3I = 1;
        DTCON2bits.DTS2A = 1;
        DTCON2bits.DTS2I = 1;
        DTCON2bits.DTS1A = 1;
        DTCON2bits.DTS1I = 1;

// FBORPOR register
//      _HPOL = 0;                          // The high bits have active low polarity
```

```
}


void Initialization(void)
{                                                                    // 2.1) Initialize LEDs
        LATAbits.LATA9 = 0;
        LATAbits.LATA10 = 0;
        LATAbits.LATA14 = 0;
        LATAbits.LATA15 = 0;

        d1 = 0;
        d2 = 0;
        d0 = 0;

        PWMfact = 14.58;

        LATDbits.LATD11 = 0;

        flag1 = 0;

/* Initialising indexes*/
// Recall that when i=1200 (ie i=120 deg) then j=600 (ie j=60 deg) and k=0 (k=0 deg) */
// Therefore, when i=0 degrees, j=300 degrees and k=240 degrees.
        i = 0;                                                       // Start with i=0 degrees

        j = 3000;                                                    // j=300 degrees
        k = 2400;                                                    // k=240 degrees
        w = 60;                                                      // Implement a 1 Hz sinusoid
        phi = 0;                                                 // Start the angle at zero
        m = 717;                                                     // Implement a modulation index of
0.7
```

```
        // Implement the calculated duty cycle
//      PDC1 = (int)(PWMfact*duty1);
//      PDC2 = (int)(PWMfact*duty2);
//      PDC3 = (int)(PWMfact*duty3);

}

/* Space Vector Modulation (SVM) Algorithm */
// 8 inverter states (including 2 zero states) described by a vector rotating anticlockwise at fout Hz (where usually fout ~ 60Hz)
// View six non-zero states as six segments of a circle. Each segment has a different way to compute the duty cycle
void CalculateDuty(void)
{
        if (phi < 60)
        {
                d1 = m*(cos_minus_ksin_1024_table[i]);
                d2 = m*(cos_minus_ksin_1024_table[k]) ;//d2 = m*(k2sin_1024_table[i]);
                d0 = ((long)1048576)-d1-d2;                    //2^20 = 1048576 (shifts values to left so that whole numbers can be used, not floats

                P1 = d0/4;
                P2 = d1/2+d0/4;
                P3 = d1/2+d2/2+d0/4;
        }
        else if (phi < 120)
        {
                d1 = m*(cos_minus_ksin_1024_table[j]) ;//d1 = m*(cos_ksin_1024_table[i]);
                d2 = m*-1*(cos_minus_ksin_1024_table[i]);
                d0 = ((long)1048576)-d1-d2;
```

```
        P1 = d2/2 + d0/4;
        P2 = d0/4;
        P3 = d1/2+d2/2+d0/4;
}
else if (phi < 180)
{
        d1 = m*(cos_minus_ksin_1024_table[k]) ;//d1 = m*(k2sin_1024_table[i]);
        d2 = m*-1*(cos_minus_ksin_1024_table[j]) ;//d2 = m*-1*(cos_ksin_1024_table[i]);
        d0 = ((long)1048576)-d1-d2;

        P1 = d1/2+d2/2+d0/4;
        P2 = d0/4;
        P3 = d1/2+d0/4;
}
else if (phi < 240)
{
        d1 = m*-1*(cos_minus_ksin_1024_table[i]);
        d2 = m*-1*(cos_minus_ksin_1024_table[k]) ;//d2 = m*(-1*k2sin_1024_table[i]);
        d0 = ((long)1048576)-d1-d2;

        P1 = d1/2+d2/2+d0/4;
        P2 = d2/2+d0/4;
        P3 = d0/4;
}
else if (phi < 300)
{
        d1 = m*-1*(cos_minus_ksin_1024_table[j]) ;//      d1 = m*-1*(cos_ksin_1024_table[i]);
        d2 = m*(cos_minus_ksin_1024_table[i]);
        d0 = ((long)1048576)-d1-d2;

        P1 = d1/2+d0/4;
        P2 = d1/2+d2/2+d0/4;
```

```
            P3 = d0/4;
        }
        else
        {
            d1 = m*-1*(cos_minus_ksin_1024_table[k]) ;//d1 = m*(-1*k2sin_1024_table[i]);
            d2 = m*(cos_minus_ksin_1024_table[j]) ;//d2 = m*(cos_ksin_1024_table[i]);
            d0 = ((long)1048576)-d1-d2;

            P1 = d0/4;
            P2 = d1/2+d2/2+d0/4;
            P3 = d2/2+d0/4;
        }

        P1 = 737*P1;            //similar to modulation index - changes amplitude of output voltage
        P1 = P1>>18;
        PDC3 = P1;

        P2 = 737*P2;
        P2 = P2>>18;
        PDC1 = P2;

        P3 = 737*P3;
        P3 = P3>>18;
        PDC2 = P3;
}
void main(void)
{
        Configuration();                        // 1) Configure the microcontroller
        Initialization();                       // 2) Initialize the microcontroller

        while(1)
        {
```

```
if (flag1)
{

/* Reset Indexes */
// These 3 if statements are used to make the indeces return to the start of the look-up table
// This will happen at different times for each variable, as they are 60 degrees out of phase

        if (phi >= 360)
        {
                phi = 0;
                i = 0;
        }

        if (j >= 3600)
        {
                j = 0;
        }

        if (k >= 3600)
        {
                k = 0;
        }

        CalculateDuty();  // Implement the SVM Algorithm

        phi = phi + 1.2;   // NOTE: We can make the phi increment smaller to increase resolution
                                                        // we can make any delta_phi =k*0.1 where k
is any integer
        i = i + 12;                     //i = i+12 for 60Hz
        j = j + 12;
        k = k + 12;
```

```
                    flag1 = 0;
                }
            }
        }
```

B. PCB design of the L-C-L filter

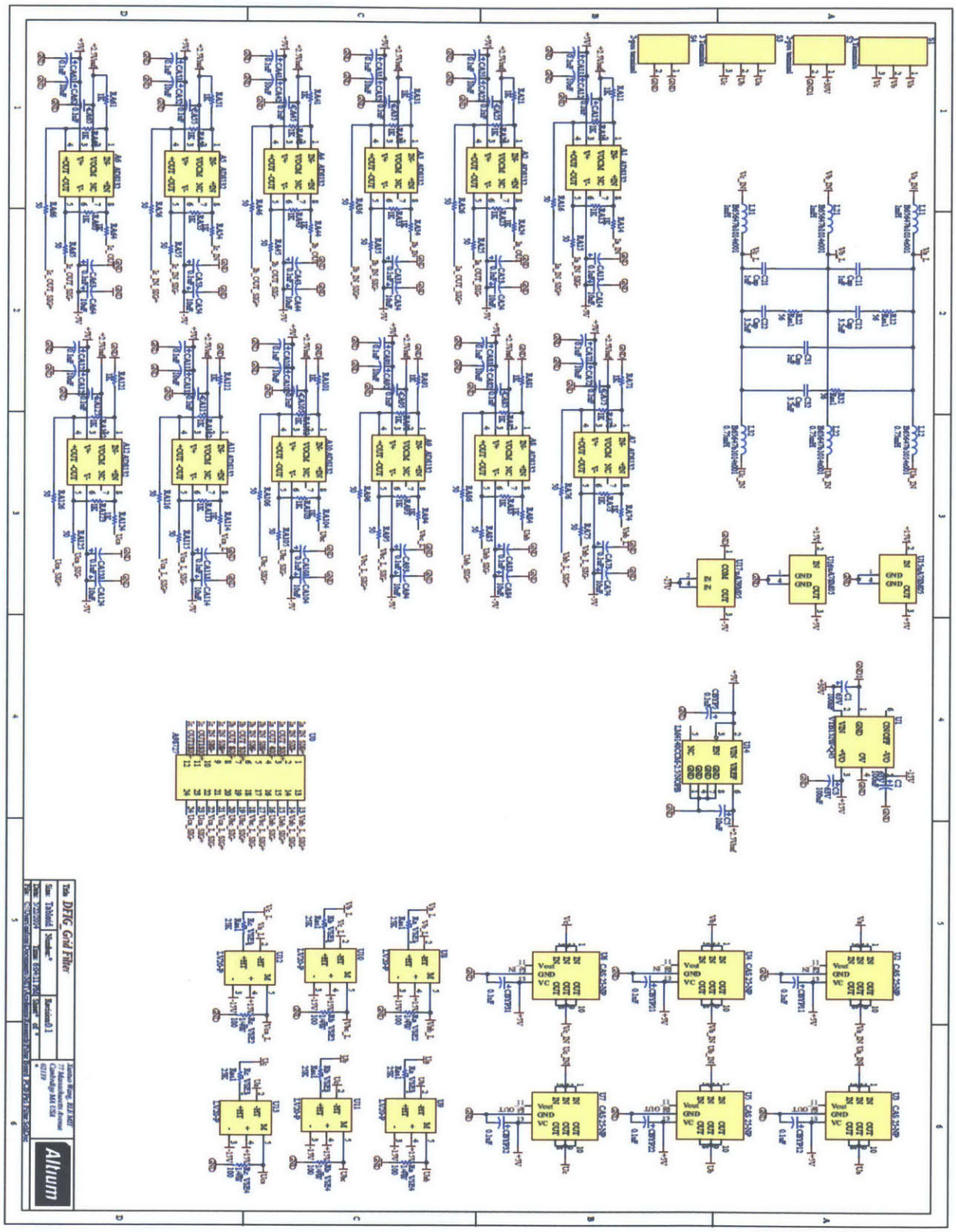

Figure 37. Grid filter design schematics.

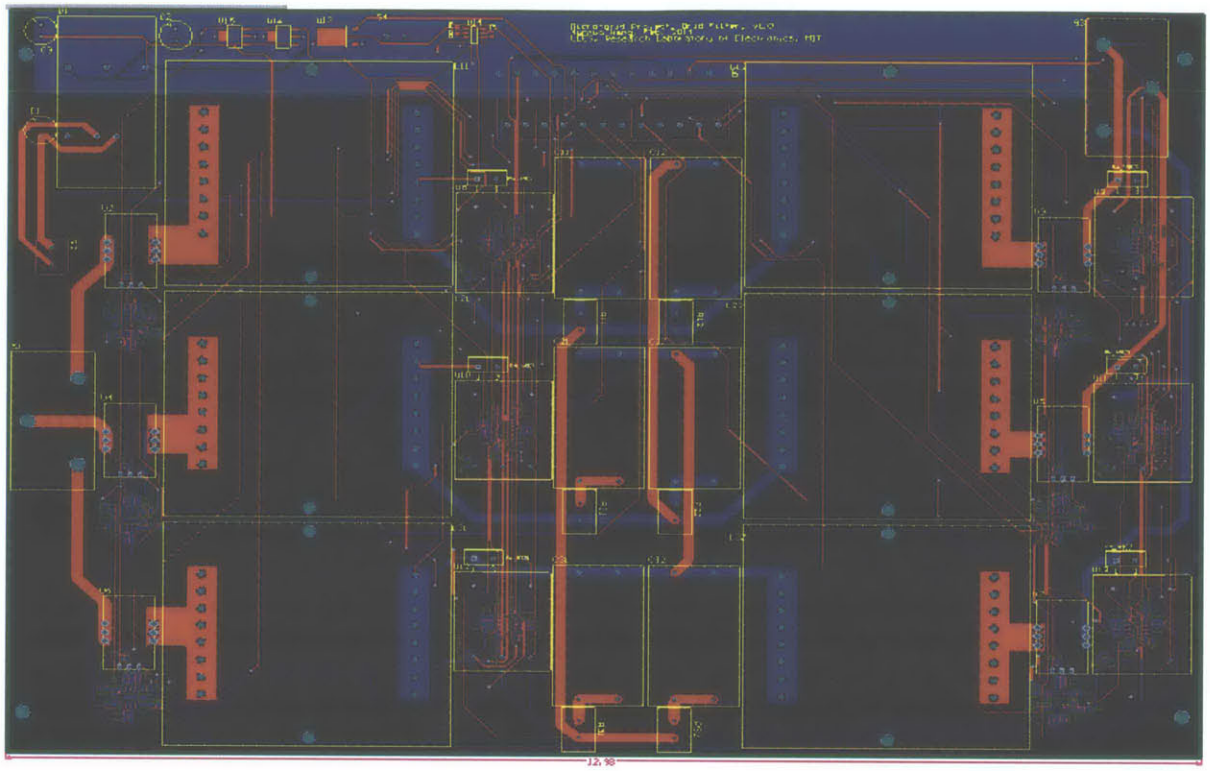

Figure 38. PCB of grid filter in 2D view.

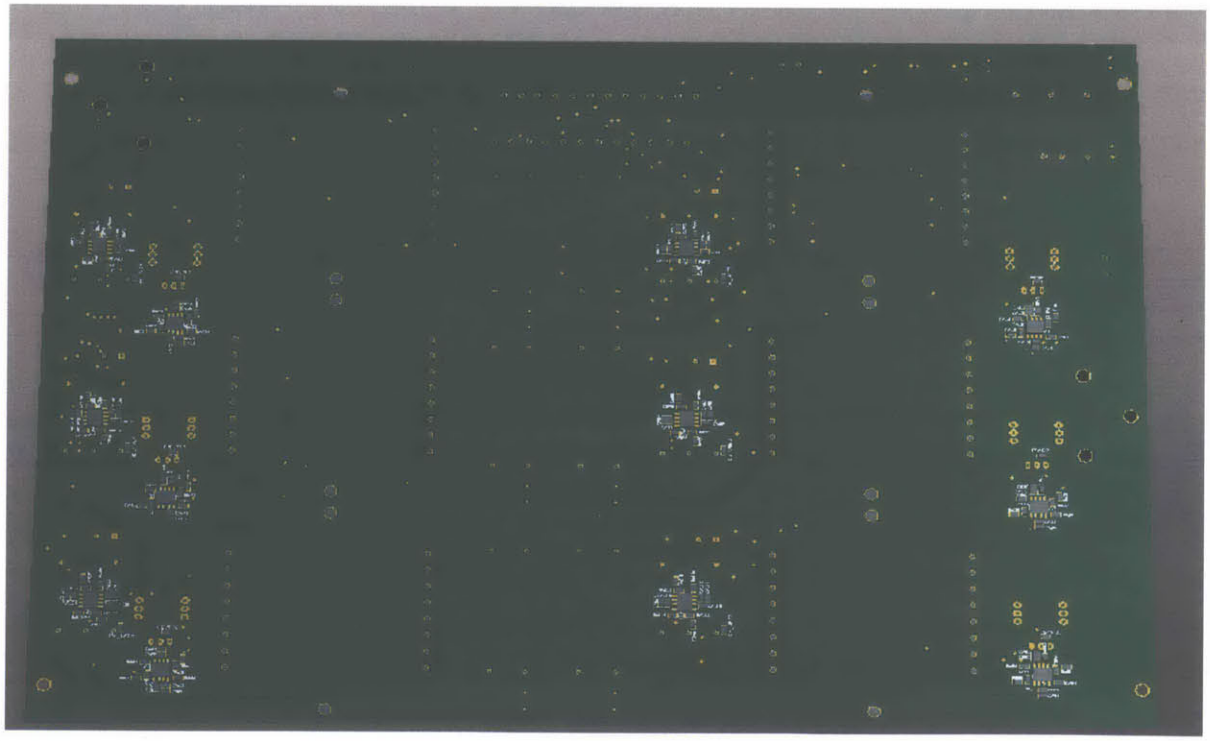

(a) Its 3D view (bottom)

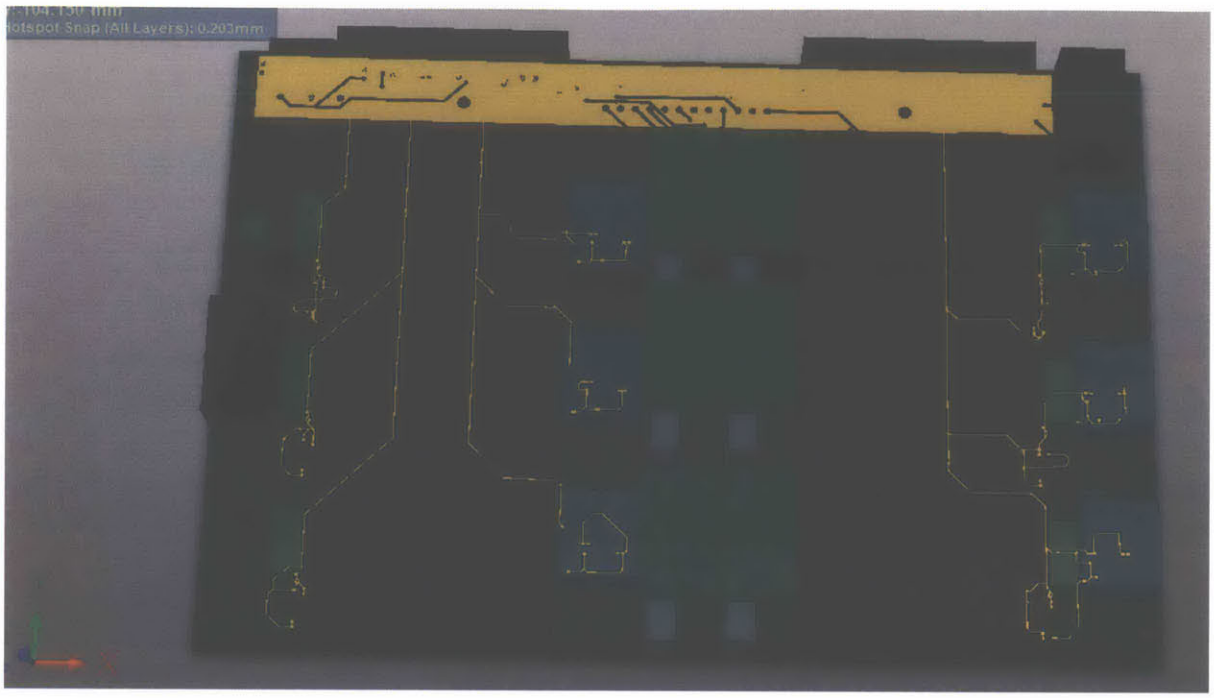

(b) Its 3D view highlighting the ground tracing (top)

Figure 39. PCB of grid filter in 3D view.

C. Construction of the filter inductors

Figure 40. Inductor build materials: 16AWG coil, inductor core, and mounting assembly.

Figure 41. Inductor coil winding process.

Bibliography

[1] R. Teodorescu, M. Liserre, P. Rodriguez, Grid Converters for Photovoltaic and Wind Power Systems, Wiley, 2011.

[2] M. P. Papadopoulos, S. A. Papathanassiou, N. G. Boulaxis, and S. T. Tenzarakis, "Voltage quality change by grid-connected wind turbines," in European Wind Energy Conference, Nice, France, 1999, pp. 783-785.

[3] J. L. Kirtley Jr., "Electric Power Principles: Sources, Conversion, Distribution and Use", Wiley, Sep. 2012.

[4] A. E. Fitzgerald, Charles Kingsley Jr., Stephen Umans, "Electric Machinery", McGraw-Hill Science, July 2002.

[5] P. C. Krause, O. Wasyczuk, S. D. Sudhoff, "Analysis of Electric Machinery and drive systems", Wiley, 2002.

[6] H. Bai, A. Taylor, W. Guo, G. Szatmari-Voicu, N. Wang, J. Patterson, J. Kane, "Design of an 11kW power factor correction and 10kW ZVS DC/DC converter for a high-efficiency battery charger in electric vehicles", IET Power Electronics 2012, pp. 1-9.

[7] H.H. Zeineldin, J.L. Kirtley, "Micro-grid operation of inverter based distributed generation with voltage and frequency dependent loads", IEEE Power & Energy Society General Meeting, 2009, pp. 1-6.

[8] H. Grotstollem, A. Bunte, "Control of Induction Motor with Orientation on Rotor Flux or on Stator Flux in a very wide Field Weakening Region-Experiment Results", Industrial Electronics, 1996. ISIE'96., Proceedings of the IEEE International Symposium on. Vol. 2. IEEE, 1996.

[9] I. Takahashi and T. Noguchi, "A new quick-response and high-efficiency control strategy of an induction motor," IEEE Transcation on Industry Application, Vol. IA-22, Sep/Oct., 1986, pp. 820-727.

[10] A. Banerjee, M. S. Tomovich, S. B. Leeb, J. L. Kirtley, "Control Architecture for a Doubly-fed Induction Machine Propulsion Drive", IEEE APEC 2013.

[11] R. H. Lasseter, P. Paigi, "Micro-grid: A Conceptual Solution", 35th Annual IEEE Power Electronics Specialists Conerence, Vol. 6, 2004, pp. 4285-4290.

[12] A. Gupta, S. N. Singh, D. K. Khatod, "Modeling and Simulation of Doubly Fed Induction Generator Coupled With Wind Turbine-An Overview", Journal of Engineering, Computers & Applied Sciences, vol. 2, No.8, August 2013.

[13] A. Kwasinski, "Quantitative Evaluation of DC Microgrids Availability: Effects of Systems Architecture and Converter Topology Design Choices", IEEE Trans. On Power Electronics, Vol. 26, No. 3, March 2011.

[14] J. Liang, C. Feng, "Stability Improvement of Micro-grids with Coordinate Control of Fuel Cell and Ultracapacitor", Power Electronics Specialists Conference 2007, pp. 2472-2477.

[15] J. Et, R. Lasseter, B. Schenkman, J. Stevens, D. Klapp, H. Volkommer, E. Linton, H. Hurtado, J. Roy, "Overview of the CERTS Microgrid Laboratory Test Bed", Integration of Wide-Scale Renewable Resources into the Power Delivery System, 2009 CIGRE/IEEE PES Joint Symposium, pp. 1, 2009.

[16] ABB IEC Low Voltage AC Motors/General Performance Motors/IE1 Standard Efficiency Cast Iron Motors, Technical catalog, available at:

[17] IEEE Standard for Interconnecting Distributed Resources with Electric Power systems, IEEE Std 1547 – 2003, June 2003.

[18] N. Pogaku, M. Prodanovic, T.C. Green, "Modeling Analysis and Testing of Autonomous Operation of an Inverter-Based Microgrid,", IEEE Trans. Power Electronics, vol. 22, No. 2, pp.613-625, Mar 2007.

[19] R. Teodorescu, M. Liserre, P. Rodriguez, Grid Converters for Photovolatic and Wind Power Systems, UK: Wiley, 2011, p. 289-311.

[20] IEEE Recommended Practice for Excitation System Models for Power System Stability Studies, IEEE Std 421.5 – 2005, April 2006.

[21] G. Abad, M. A. Rodriguez, J. Poza, J. M. Canales, "Direct Torque Control for Doubly Fed Induction Machine-Based Wind Turbines Under Voltage Dips and Without Crowbar Protection," IEEE Transactions on Energy Conversion, Vol. 25, No. 2, June 2010.

[22] Z. Liu, O.A. Mohammed, S. Liu, "A Novel Direct Torque Control of Doubly-Fed Induction Generator Used for Variable Speed Wind Power Generation," IEEE 2007, 1-4244-129806.

[23] Pérez-Arriaga, I.J., "Regulation of the power sector." Springer, 2013.

[24] A.H. Kasem Alaboudy, H.H. Zeineldin, J.L. Kirtley, "Microgrid Stability Characterization Subsequent to Fault-Triggered Islanding Incidents", IEEE Trans. On Power Delivery, vol. 27, No. 2, pp. 658-669, Apr 2012.